Chem Soc Rev

REVIEW ARTICLE

View Article Online
View Journal | View Issue

Cite this: *Chem. Soc. Rev.*, 2014, 43, 5766

Adsorptive separation on metal–organic frameworks in the liquid phase

Ben Van de Voorde,[a] Bart Bueken,[a] Joeri Denayer[b] and Dirk De Vos*[a]

Received 2nd January 2014

DOI: 10.1039/c4cs00006d

www.rsc.org/csr

While much attention of the MOF community has been devoted to adsorption and purification of gases, there is now also a vast body of data on the capability of MOFs to separate and purify liquid mixtures. Initial studies focused on separation of petrochemicals in apolar backgrounds, but the attention has moved now to the separation of complex, *e.g.* chiral compounds, and to the isolation of biobased compounds from aqueous media. We here give an overview of most of the existing literature, with an accent on separation mechanisms and structure–selectivity relationships.

1. Introduction

In the chemical, petrochemical and pharmaceutical industries separation technology is a key element in the production of pure compounds. A large portion of the production costs are associated with purification steps, for instance using solvent extraction, adsorption, crystallization and distillation processes.[1,2] Presently, distillation accounts for more than 90% of all separation processes in the chemical industry.[3] Due to the reactive nature or the decomposition of certain chemicals and the high costs associated with distillation, valid alternatives are needed for a sustainable chemical industry in the future.[4] Adsorptive separation is such a promising alternative; it is already used in a multitude of processes in industry today.[5] An adsorbent is able to separate a mixture of chemicals into pure compounds, mostly based on differences in the interaction between the adsorbent and the constituents of the mixture.[6] The efficiency of separation is therefore strongly determined by the characteristics of the adsorbent. Microporous materials such as zeolites,[3] activated carbon,[7] carbon molecular sieves,[8] aluminophosphates,[9] inorganic or polymeric resins[10] and composite materials[11] have already been studied intensively for adsorptive separations. However, in order to realise the challenging separations of future industries, superior adsorbents are still needed. Certain metal-organic

[a] *Centre for Surface Chemistry and Catalysis, KU Leuven, Arenbergpark 23, B-3001 Leuven, Belgium. E-mail: Dirk.DeVos@biw.kuleuven.be; Fax: +32 16 321998; Tel: +32 16 321639*
[b] *Department of Chemical Engineering, Vrije Universiteit Brussel, Pleinlaan 2, B-1050 Elsene, Belgium*

Ben Van de Voorde

Ben Van de Voorde (1988) obtained his BSc (2009) and MSc (2011) in Bioscience Engineering at the KU Leuven in Belgium. After joining the group of Prof. Dirk De Vos in 2011, he received a grant in 2012 from the Science foundation Flanders (FWO) to conduct research in the Solid Mechanics and Materials Engineering Group at the University of Oxford under the supervision of Dr Jin-Chong Tan. His current doctoral research interests at the Center for Surface Chemistry and Catalysis (COK) include liquid phase adsorption and catalysis with metal–organic frameworks.

Bart Bueken

Bart Bueken (1989) obtained his BSc (2010) and MSc (2012) in Bioscience Engineering from the KU Leuven in Belgium. In 2013 his master's thesis on the influence of synthesis modulation on the catalytic activity of UiO-66 was awarded the prestigious Umicore scientific award. After his studies he received a fellowship grant from the Science Foundation Flanders (FWO) and started his PhD at the Center for Surface Chemistry and Catalysis (COK) in the group of Prof. Dirk De Vos. His current research interests include the synthesis of and catalysis with metal–organic frameworks.

frameworks (MOFs) which combine high chemical and thermal stability,[12–14] large surface areas[15,16] and tuneable surface properties[17–21] could be valuable candidates in this respect. MOFs are hybrid materials constructed from inorganic metal nodes and multidentate organic ligands organised in a crystalline three-dimensional network.[22] Consequently, well-defined pore size distributions are obtained making MOFs good candidates for liquid phase adsorptive separations.[23,24] In this review, we will discuss separations with MOFs in the liquid phase. More specifically the focus will be directed to two different solvent conditions, *viz.* the organic phase and the aqueous phase. Especially aqueous phase separations are considered more challenging, due to stability issues of many MOFs in water.[25,26] Nevertheless, a steep rise in demand for adsorptive separations from the aqueous phase can be anticipated for the future (bio-)sustainable chemical industry, in which biomass will play a key role and distillation will not always be an energetically favourable or chemically feasible option.[27] Although MOFs have not yet found their way into industrial separation applications today, it is clear that they show great potential for liquid phase adsorption processes.

2. Separations from the organic phase

2.1 Fuel upgrading

The removal of N/S-compounds from fossil fuels remains a topical research area, due to the stringent regulations imposed by governments. As the current catalytic hydrodesulfurization (HDS) and hydrodenitrogenation (HDN) technologies alone are not capable of meeting the requirements needed in the future (*e.g.*, <5 ppm S), adsorptive desulfurization and denitrogenation offer an attractive solution.[28] Tables 1 and 2 summarize the MOFs that have been tested in adsorptive desulfurization and denitrogenation.

Desulfurization. The sulfur compounds commonly found in diesel and gasoline fuels are thiophene (TP), benzothiophene (BT), dibenzothiophene (DBT) and alkylsubstituted dibenzothiophenes (*e.g.* 4,6-dimethyl-DBT, DMDBT) (Fig. 1). Especially the latter are very difficult to remove with HDS and their removal using a solid Co–Mo or Ni–Mo catalyst[1] is accompanied by a substantial loss in octane and decane number.[29] For the adsorptive removal of sulfur compounds from hydrocarbon streams, the main challenge is designing an adsorbent capable of selectively removing sulfur compounds at very low concentrations from a complex mixture of paraffins and aromatics. As novel sorbents, the use of MOFs for adsorptive desulfurization was pioneered by Matzger and coworkers.[30] The removal of thiophenic sulfur compounds from an isooctane hydrocarbon stream was tested with five MOFs, *viz.* the prototypical MOF-5 and HKUST-1 alongside MOF-177, MOF-505 and UMCM-150. MOF-5 and MOF-177 are both materials constructed from $Zn_4O(COO)_6$ secondary building units (SBUs). In MOF-5 these SBUs are interconnected by terephthalate linkers (1,4-benzenedicarboxylates, BDC) forming a cubic **pcu** topology. In MOF-177 the SBUs are linked by 1,3,5-benzenetribenzoates (BTB). HKUST-1, MOF-505 and UMCM-150 are Cu paddlewheel MOFs, with 1,3,5-benzenetricarboxylates (BTC), 3,3′,5,5′-biphenyltetracarboxylates

Joeri Denayer

Joeri Denayer (1971) is professor at the Department of Chemical Engineering at the Vrije Universiteit Brussel, Belgium. He obtained his PhD in Applied Sciences from the Vrije Universiteit Brussel in 1998. After obtaining his PhD, he conducted research in the field of catalysis for petroleum refining and petrochemistry for TOTAL. After 3 years in industry, he returned to academia. Currently, his research focuses on adsorption, diffusion and molecular separation in porous materials, from the fundamental level to the application. This includes the experimental study of adsorption, modeling of separation and catalytic processes, development of high-throughput experimental techniques to study gas- and liquid-phase multicomponent adsorption, analysis of structure–selectivity relationships in adsorption, development of micro-separators and process intensification. His research was awarded with the DSM-Award for chemistry and technology and the EXXONMOBIL Chemical European Science & Engineering Award.

Dirk De Vos

Dirk De Vos (1967) is a full professor in Bioscience Engineering at KU Leuven (Belgium). He completed his master's and PhD education at KU Leuven, and was a post-doc at Purdue University with Thomas Bein. His main interest is in porous materials, such as zeolites, layered double hydroxides and MOFs, in the interactions of organic molecules with these materials, and in catalytic transformations inside the pores. Together with J. Hofkens and M. Roeffaers, he pioneered the visualisation of active sites in porous materials by light microscopic techniques. His team made groundbreaking discoveries in the application of metal–organic frameworks to liquid phase separation and catalysis, and in the shaping of MOFs as films or patterns. His awards include the BASF Catalysis Award and the D. W. Breck Award of the International Zeolite Association.

Table 1 Overview of MOFs applied in adsorptive desulfurization

MOF	Solvent	Maximum uptake of sulfur compounds (wt% S)				Ref.
		TP	BT	DBT	DMDBT	
HKUST-1	Isooctane	—	2.5	4.5	1.6	30
	Isooctane/toluene (85/15)	—	—	1.0	0.8	31
	n-Octane/toluene (95/5)	8.0	—	—	—	33
	2,2,4-Trimethylpentane	—	4.0	4.5	1.4	34
	H/T (80/20)	3.8	2.4	2.1	—	35
	H/T (20/80)	1.9	0.5	0.4	—	35
UMCM-150	Isooctane	—	4.0	8.3	4.1	30
	Isooctane/toluene (85/15)	—	—	2.5	0.7	31
MOF-505	Isooctane	—	5.1	3.9	2.7	30
	Isooctane/toluene (85/15)	—	—	3.3	0.9	31
MOF-5	Isooctane	—	1.6	3.3	1.4	30
	Isooctane/toluene (85/15)	—	—	1.0	0.7	31
MOF-177	Isooctane	—	0.8	1.8	0.8	30
CPO-27(Ni)	*n*-Octane/toluene (95/5)	9.6	—	—	—	33
	H/T (20/80)	4.6	4.5	3.5	—	35
CPO-27(Co)	H/T (20/80)	4.9	4.8	3.5	—	35
Cu_3(NAPANA)	Isooctane	—	2.8	3.3	—	36
rho-ZMOF	*n*-Octane/toluene (95/5)	1.3	—	—	—	33
ZIF-8	*n*-Octane/toluene (95/5)	1.0	—	—	—	33
ZIF-76	*n*-Octane/toluene (95/5)	1.9	—	—	—	33
MIL-53(Al) (A100)	2,2,4-Trimethylpentane	—	—	3.8	—	34
MIL-53(Al)	H/T (80/20)	<0.4	—	<0.2	—	35
	H/T (20/80)	<0.4	—	<0.2	—	35
	n-Octane	—	0.9	—	—	37
	n-Octane/toluene (75/25)	—	0.5	—	—	37
MIL-53(Al)/$CuCl_2$	*n*-Octane	—	0.8	—	—	37
	n-Octane/toluene (75/25)	—	0.4	—	—	37
MIL-53(Cr)	*n*-Octane	—	2.4	—	—	37
	n-Octane/toluene (75/25)	—	0.9	—	—	37
MIL-53(Cr)/$CuCl_2$	*n*-Octane	—	1.9	—	—	37
	n-Octane/toluene (75/25)	—	0.8	—	—	37
MIL-53(Fe) hydrated	Heptane	—	3.6	—	—	38
	Isopropanol	—	11.2	—	—	38
MIL-53(Fe) dehydrated	Heptane	—	5.3	—	—	38
	Isopropanol	—	7.4	—	—	38
MIL-47(V)	H/T (80/20)	<0.4	—	<0.2	—	35
	H/T (20/80)	<0.4	—	<0.2	—	35
	n-Octane	—	5.7	—	—	37
	n-Octane/toluene (75/25)	—	1.2	—	—	37
MIL-47(V)/$CuCl_2$	*n*-Octane	—	7.4	—	—	37, 39
	n-Octane/toluene (75/25)	—	1.4	—	—	37
MIL-100(Fe)	2,2,4-Trimethylpentane	—	—	2.5	—	34
	Heptane	3.2	—	—	—	40
	H/T (80/20)	1.5	1.4	1.2	—	35
	H/T (20/80)	0.4	<0.2	<0.2	—	35
MIL-100(Al)	Heptane	3.4	—	—	—	40
	H/T (80/20)	0.8	1.4	1.0	—	35
	H/T (20/80)	<0.4	0.2	<0.2	—	35

Table 1 (*continued*)

MOF	Solvent	Maximum uptake of sulfur compounds (wt% S) TP	BT	DBT	DMDBT	Ref.
MIL-100(V) vac	Heptane	1.9	—	—	—	40
MIL-100(Cr)	Heptane	2.7	—	—	—	40
	H/T (80/20)	0.8	1.7	1.2	—	35
	H/T (20/80)	<0.4	<0.2	0.2	—	35
MIL-101(Cr)	H/T (80/20)	1.2	1.2	1.4	—	35
	H/T (20/80)	0.4	<0.2	0.2	—	35
	Gas oil	—	—	0.5	—	41
	Isooctane	—	—	1.7	1.1	41
	*n*O*p*X	—	0.7	—	—	42
MIL-101(Cr)/1% PWA	*n*O*p*X	—	0.6	—	—	42
MIL-101(Cr)/ED	*n*O*p*X	—	0.6	—	—	43
MIL-101(Cr)/AMSA	*n*O*p*X	—	0.7	—	—	43
MIL-101(Cr)/0.25% GO	*n*O*p*X	—	0.7	—	—	44

H/T (80/20) = heptane/toluene 80/20 v/v; H/T (20/80) = heptane/toluene 20/80 v/v; *n*O*p*X = *n*-octane/*p*-xylene 25/75 v/v; PWA = phosphotungstic acid; ED = ethylenediamine grafted; AMSA = aminomethanesulfonic acid grafted; GO = graphene oxide; vac = MIL-100(V) pretreated under vacuum at 423 K for 12 h; TP = thiophene; BT = benzothiophene; DBT = dibenzothiophene; DMDBT = 4,6-dimethyldibenzothiophene.

and biphenyl-3,4′,5-tricarboxylates as linkers respectively. The latter also features the trinuclear $Cu_3(CO_2)_6$ SBU besides the $Cu_2(CO_2)_4$ paddlewheels. All three Cu materials were found to be superior to the Zn frameworks. MOF-505 even outperformed the capacity of the benchmark NaY zeolite at low concentrations by a factor of ten, adsorbing up to 2.5 wt% S (BT) and 1.7 wt% S (DBT) from isooctane. The authors did not find a clear correlation between the surface area and the amount of S adsorbed at saturation; however they noted that the frameworks with the highest uptake (UMCM-150 and MOF-505) both have coordinatively unsaturated Cu-metal sites. The Matzger group published a follow-up study by introducing an aromatic compound in the solvent, mimicking a diesel fuel.[31] The presence of these aromatic compounds induces extra competition for possible adsorption sites. Single compound adsorption isotherms for BT and DMDBT out of isooctane/toluene (85 : 15 – v : v) clearly show a dramatic loss in affinity compared to the isotherms without toluene in the solvent mixture. At the equilibrium concentration of 500 ppmw S (BT), UMCM-150 had an uptake of 5 wt% S from isooctane, while only 1 wt% S was adsorbed out of isooctane/toluene. This loss in affinity clearly proves that dispersion interactions play a major role in the interaction between either toluene or the aromatic heterocycles and the framework. Nevertheless, UMCM-150 was still able to adsorb up to 2.4 wt% S (DBT) in a breakthrough experiment with a spiked diesel sample, making it a superior material compared to activated carbon and zeolites.[31]

The use of MOFs with coordinatively unsaturated sites (CUS) for adsorptive desulfurization was further explored by Peralta *et al.* and Achmann *et al.*[32,33] In the study of Peralta *et al.*, HKUST-1 and CPO-27(Ni), a honeycomb-like framework made up of chains of edge-sharing NiO_5(CUS)-octahedra linked by 2,5-dihydroxyterephthalates, were found to be selective for the adsorption of thiophene over toluene. The authors did not link the high selectivity of the MOFs with CUS to a possible sulfur–metal interaction, but stated that an electrostatic interaction between the electric field generated by the framework and the dipole moment of the aromatic molecules is the most plausible explanation for this selectivity. Achmann *et al.* concluded that HKUST-1 is a very promising adsorbent for adsorptive desulfurization combining fast kinetics with decent capacities. The first authors to link the strong adsorption affinity and high selectivity for sulfur compounds to CUS were Blanco-Brieva *et al.*[34] They stated that the significantly higher uptake of sulfur compounds by commercially available HKUST-1 (Basolite C300) compared to Basolite F300 (Fe-BTC) and Basolite A100 (MIL-53(Al)) was due to a much stronger S-atom interaction with the open Cu sites. Also the copper paddlewheel-based material Cu_3(NAPANA), constructed from Cu-paddlewheels and NAPANA (Fig. 2), was found to be very effective in adsorption of BT and DBT out of an isooctane background, due to a strong sulfur–metal coordination and dispersion interactions between the π-electrons of the thiophenes and the π-electrons of the structure.[36] Cu_3(NAPANA) was able to adsorb 2.8 wt% S for BT and 3.5 wt% S for DBT at saturation and the total capacity was not altered during consecutive runs.

An alternative approach to MOFs with structural open metal sites is the postsynthetic incorporation of transition metals in the pores after the synthesis. The vanadium terephthalate MIL-47, consisting of one-dimensional lozenge shaped channels formed by the interconnection of chains of vertex-sharing VO_6 octahedra through terephthalate linkers, showed a remarkable adsorption capacity for benzothiophene out of *n*-octane when loaded with $CuCl_2$.[39] The loading of the framework with $CuCl_2$ and the ensuing reduction of Cu^{2+} to Cu^{+} during the low

Table 2 Overview of MOFs applied in adsorptive denitrogenation

		Maximum uptake of nitrogen compounds (wt% N)							
MOF	Solvent	IND	2MI	1,2DMI	CBZ	NMC	BTZ	QUI	Ref.
MIL-100(Fe)	H/T (80/20)	4.3	3.2	2.6	—	1.5	—	—	35
	H/T (20/80)	1.9	—	0.9	—	0.2	—	—	35
	Heptane	5.4	—	2.6	—	—	—	—	40
MIL-100(Cr)	H/T (80/20)	4.4	3.1	2.6	—	1.5	—	—	35
	H/T (20/80)	1.9	—	0.8	—	0.2	—	—	35
	Heptane	4.8	—	3.0	—	—	—	—	40
	*n*Op*X*	1.2	—	—	—	—	—	3.7	43
MIL-100(Cr)/ED	*n*Op*X*	1.1	—	—	—	—	—	1.3	43
MIL-100(Cr)/AMSA	*n*Op*X*	1.2	—	—	—	—	—	3.5	43
MIL-100(Al)	H/T (80/20)	4.1	3.1	2.4	—	1.3	—	—	35
	H/T (20/80)	1.6	—	0.7	—	0.2	—	—	35
	Heptane	7.1	—	2.4	—	—	—	—	40
MIL-100(V) vac	Heptane	5.4	—	2.4	—	—	—	—	40
MIL-101(Cr)	H/T (80/20)	4.8	3.6	2.4	—	2.1	—	—	35
	H/T (20/80)	1.7	—	0.7	—	0.3	—	—	35
	Isooctane	2.3	—	—	—	—	—	—	41
	Gas oil	2.3	—	—	0.5	—	—	—	41
	*n*Op*X*	2.9	—	—	—	—	—	5.2	44
MIL-101(Cr)/1% PWA	*n*Op*X*	1.8	—	—	—	—	—	3.0	42
MIL-101(Cr)/0.25% GO	*n*Op*X*	3.8	—	—	—	—	—	6.0	44
HKUST-1	H/T (80/20)	2.6	1.8	—	—	0.3	—	—	35
	H/T (20/80)	1.6	—	0.3	—	<0.1	—	—	35
CPO-27(Ni)	H/T (20/80)	1.3	—	0.4	—	<0.1	—	—	35
CPO-27(Co)	H/T (20/80)	1.2	—	0.4	—	<0.1	—	—	35
MIL-47(V)	H/T (80/20)	<0.1	<0.1	<0.1	—	<0.1	—	—	35
	H/T (20/80)	<0.1	<0.1	<0.1	—	<0.1	—	—	35
MIL-53(Al)	H/T (80/20)	<0.1	<0.1	<0.1	—	<0.1	—	—	35
	H/T (20/80)	<0.1	<0.1	<0.1	—	<0.1	—	—	35
MIL-53(Fe) (hydrated)	Heptane	0.7	—	—	—	—	6	—	38
	Isopropanol	0	—	—	—	—	2.9	—	38
MIL-53(Fe) dehydrated	Heptane	2.6	—	—	—	—	6.1	—	38
	Isopropanol	0	—	—	—	—	5.0	—	38

H/T (80/20) = heptane/toluene 80/20 v/v; H/T (20/80) = heptane/toluene 20/80 v/v; *n*Op*X* = *n*-octane/*p*-xylene 25/75 v/v; ED = ethylenediamine grafted; AMSA = aminomethanesulfonic acid grafted; vac = MIL-100(V) pretreated under vacuum at 423 K for 12 hours; PWA = phosphotungstic acid; GO = graphene oxide; IND = indole; 2MI = 2-methylindole; 1,2DMI = 1,2-dimethylindole; CBZ = carbazole; NMC = *N*-methylcarbazole; BTZ = benzothiazole; QUI = quinoline.

temperature pretreatment doubled the adsorption capacity to 3.1 wt% S (BT) compared to the unmodified MIL-47. The Cu-loaded MIL-47 material outperformed the Cu-loaded isostructural MIL-53(Cr) and MIL-53(Al), as no Cu^{2+} reduction was possible in the Cr and Al materials.[37] Loading MOF-5 with $Mo(CO)_6$ also proved to be a successful approach to increase the adsorption capacity for thiophenic compounds.[45] Different loadings of Mo up to 20 wt% were investigated. When MOF-5 was charged with 1.2 wt% Mo, the highest breakthrough capacities for benzothiophene were achieved. The adsorption capacity was not proportional to the Mo content, probably due to pore blockage and inaccessible Mo species at higher Mo loadings. The authors also investigated the influence of aromatic species on the adsorption performance of the MOF-5/$Mo(CO)_6$, and concluded that there was a significant performance loss associated with competition of aromatics. The DBT breakthrough capacity of MOF-5/$Mo(CO)_6$ decreased by approximately 90% compared to the capacity with low concentrations of benzene in the feed. Similar decreased breakthrough capacities were found for other π-complexing adsorbents, like Cu(I)–Y zeolite, when benzene was present in the feed.[29]

The regenerability of an adsorbent after desulfurization is of paramount importance for possible use in industry. Therefore the thermal regeneration of HKUST-1 after sulfur adsorption was investigated by treatment under a He flow at temperatures up to 473 K.[46] After the first regeneration cycle the adsorption capacity dropped dramatically (from 4.5 wt% S (DBT) to 1 wt% S (DBT)), but in further cyclic adsorption/regeneration experiments

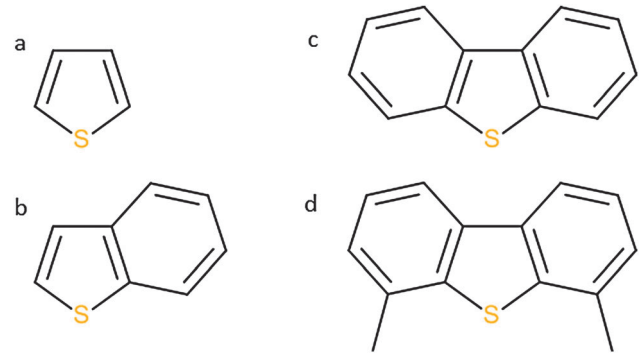

Fig. 1 Sulfur compounds commonly found in fuels: (a) thiophene; (b) benzothiophene; (c) dibenzothiophene; (d) 4,6-dimethyldibenzothiophene.

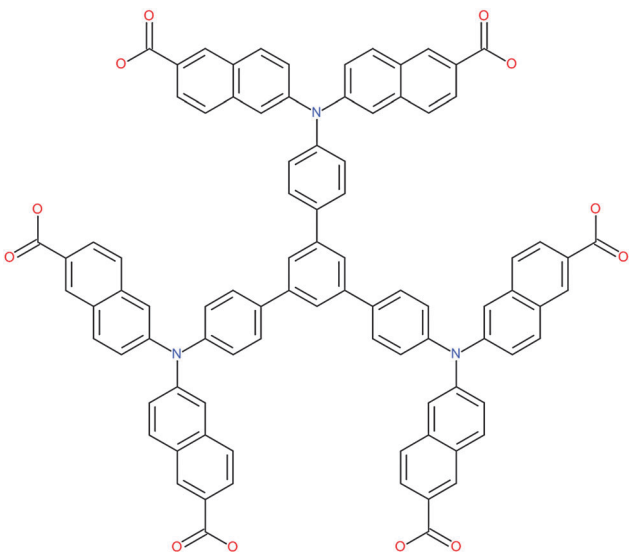

Fig. 2 NAPANA (6,6′,6″,6‴-((5′-(4-(bis(6-carboxynaphthalen-2-yl)amino)-phenyl)-[1,1′:3′,1″-terphenyl]-4,4″-diyl)bis(azanetriyl))tetrakis(2-naphthoic acid)).

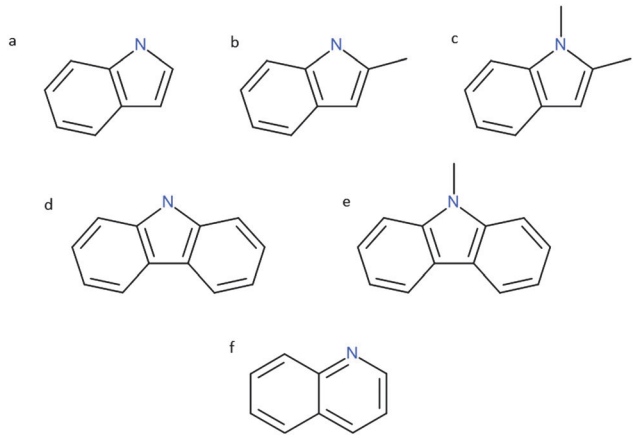

Fig. 3 Nitrogen compounds commonly found in fuels. (a) Indole; (b) 2-methylindole; (c) 1,2-dimethylindole; (d) carbazole; (e) *N*-methylcarbazole; (f) quinoline.

no changes in adsorption capacity were observed. This loss in capacity was attributed to a partial loss of the crystalline structure of the framework after the adsorption/regeneration cycle. It was concluded that the S-compounds cannot be removed by degassing the sorbent at elevated temperatures, due to the strong S–Cu interaction. A full regeneration however is possible by displacing the thiophenic compounds with a solvent like toluene, as proven in previous studies.[31,36] The use of more polar solvents like ethanol, methanol or isopropanol was investigated for the regeneration of HKUST-1 after DBT adsorption out of isopentane.[47] These studies indicated that more polar solvents have a higher efficiency for regeneration. It was found that regeneration using methanol as a solvent at room temperature is highly effective and allows full recovery of the initial adsorption capacity. After several regeneration cycles, both the crystallinity and the initial sorption capacity (5.7 wt% S (DBT)) of the HKUST-1 sorbent were essentially unchanged.

Denitrogenation. A complementary technique to reduce the S levels in fuels is to increase the efficiency of the HDS technology by removing the N-compounds that are competing for active sites on the catalyst, thereby preventing a deep HDS.[48–50] Maes *et al.* explored the use of MOFs for the selective adsorption of nitrogen compounds from simulated fuels.[35] A wide variety of MOFs, with or without open metal sites, were screened for the selective adsorption of indole (IND), 2-methylindole (2MI), 1,2-dimethylindole (1,2DMI), carbazole (CBZ), and *N*-methylcarbazole (NMC) over TP, BT, and DBT (see Fig. 3). It was found that the availability and the nature of the open metal sites are crucial factors for the adsorption of N/S-compounds. MOFs lacking open metal sites, like MIL-53(Al) and MIL-47(V), did not show any significant uptake of either S or N-compounds. Materials with hard Lewis open metal sites (Fe^{3+}, Cr^{3+}, Al^{3+}), like MIL-100 and MIL-101, showed strong uptake of N-compounds and only weak affinity for S-compounds. On the other hand, the materials exposing soft Lewis open metal sites (Cu^{2+}, Co^{2+}, Ni^{2+}), such as HKUST-1 and CPO-27, proved to be highly selective for the S-compounds even in the presence of significant fractions of aromatics (toluene). This observation is in perfect agreement with Pearson's hard–soft acid–base concept, in which the intermediate to strong bases like the N-heterocyclic compounds preferentially interact with the harder Lewis acid sites, such as Fe^{3+}, Cr^{3+} and Al^{3+}, while the weaker sulfur bases interact preferentially with the softer Lewis acid sites of HKUST-1 (Cu^{2+}) and CPO-27 (Ni^{2+} or Co^{2+}). To verify the interaction of the heteroatom with the open metal sites Mössbauer spectra of MIL-100(Fe) loaded with IND were recorded. The spectra suggest that IND affects the local environment of the Fe^{3+} species, most probably by an interaction of the free electron pair at N in IND with the available Fe sites. The authors concluded that MIL-100(Fe) is a cheap and easily regenerated material for the selective removal of N-heterocyclic compounds. Following these results, the MTN topology of MIL-100 (Fig. 4) was further investigated for denitrogenation by varying the metal cation in the isostructural MIL-100(Fe), MIL-100(Al), MIL-100(Cr) and MIL-100(V) materials.[40]

The combination of adsorption isotherms from a model fuel solution with microcalorimetric and infrared (IR) spectroscopic characterization showed a clear influence of the metal on the

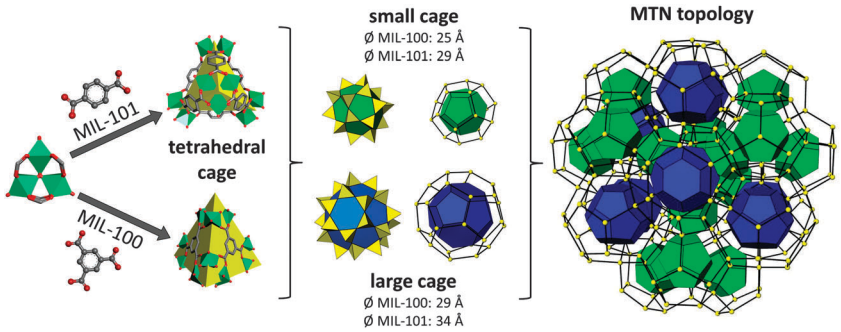

Fig. 4 MTN topology of MIL-100(M^{3+}) and MIL-101(M^{3+}). Both frameworks are built up of $M_3(\mu_3\text{-O})(COO)_6(guest)_3$ trimeric SBUs forming tetrahedral cages by interconnection with six BDC linkers (MIL-101) or four BTC linkers (MIL-100) (left). These tetrahedral cages enclose two other types of cages, one featuring only pentagonal windows ("small cage") and the other featuring pentagonal and hexagonal windows ("large cage") (center). Finally these small and large cages are stacked in an MTN topology (right).

affinity for the heterocyclic compounds and on the integral adsorption enthalpies. MIL-100(V) was found to have the highest affinity for N-compounds in combination with a low affinity for thiophenic compounds. The recorded integral adsorption enthalpies on MIL-100(V) for IND and 1,2-DMI were −158 and −198 kJ mol^{-1} respectively, compared to −20 kJ mol^{-1} for TP. IR spectra further revealed that the very strong interaction of the *N*-heterocycles was due to the coordination of the lone pair of the *N*-compounds with the open V-site and due to additional hydrogen bonding on adjacent basic sites (Fig. 5). None of the other materials showed any additional hydrogen bonding. Moreover, MIL-100(V) was easily regenerated by displacing the heterocycles with toluene without affecting the capacity or affinity of the material.

In a different study, MIL-101(Cr) was evaluated as a selective denitrogenation sorbent.[41] As the main mechanism behind the selective uptake of N-heterocycles over S-heterocycles is an enthalpic interaction with the CUS,[40] the sorption behaviour for more complex N-compounds was investigated. The adsorption selectivity for nitrogen compounds in middle-distillate oil over MIL-101 increased in the order 1,8-dimethylcarbazole ≪ carbazole < indole derivatives < indole. The authors concluded that substrate molecules with better accessibility of the N-atoms are taken up to a larger extent by MIL-101, as the coordination of N-atoms with the Cr^{3+} sites occurs more readily. Another group tried to improve the interaction of the basic N-heterocycles with the structure by loading MIL-101(Cr) with phosphotungstic acid (PWA) and evaluating the effect on the capacity.[42] MIL-101(Cr) loaded with 1 wt% PWA had a 20 wt% higher capacity compared to the virgin material for harder bases like quinoline (pK_b 9.15) in combination with a decreased uptake of BT (14 wt% less), thereby increasing the selectivity for hard N-compounds over soft S-heterocycles. Unfortunately, the incorporation of the strongly acidic PWA did decrease the affinity for softer bases like IND (pK_b 17.6), due to less favourable interaction of IND with acid sites of PWA. The effect of acidic/basic sites on the adsorptive performance of Cr-MOFs was investigated by the same group.[43] MIL-100(Cr) was post-synthetically modified with ethylenediamine and aminomethanesulfonic acid by grafting these compounds onto the Cr sites. The adsorptive removal of quinoline or BT can be improved noticeably, especially at low concentrations, with the introduction of an acidic site like in aminomethanesulfonic acid. However, the introduction of basic sites by grafting of ethylenediamine caused a severe decrease in the adsorptive performance for basic adsorbates such as quinoline. The combination of MIL-101(Cr) and graphite oxide increased the uptake of several basic nitrogen compounds by 25%.[44] The surface area of this composite was significantly increased with respect to the native MIL-101(Cr), leading to an increased and faster uptake of N-heterocycles.

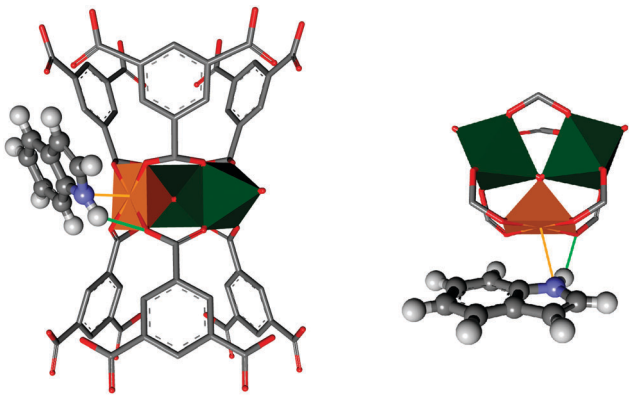

Fig. 5 Adsorption of indole on MIL-100(V): indole coordinates *via* the lone pair at N (blue) to the open V site (orange) and *via* hydrogen bonding (green) to the basic carboxylate moiety (V: green/orange; O: red; C: gray; H: white).

As an alternative to MOFs with open metal sites, flexible materials with coordinatively saturated metal cations are also potential adsorbents for N/S-compounds. The presence of open metal sites is not always advantageous due to the increased heat of adsorption, leading to higher energy consumption during adsorbent regeneration.[51] Therefore, the effect of framework flexibility on the adsorption of N/S-compounds was investigated in the breathing material MIL-53(Fe).[38] The solvent properties appeared to have a key influence on the uptake and breathing behaviour as seen by *in situ* energy-dispersive X-ray diffraction (EDXRD). The uptake of N/S-molecules by MIL-53(Fe) shows a remarkable sequence of preference, whereby strong H-bond acceptors such as benzothiazole and BT give

superior results with respect to both adsorption capacity and kinetics, compared to H-bond donors like IND. The effect is also enhanced by a specific sulfur–aromatic interaction between the S-heteroaromatic guests and the terephthalate linkers of the framework. Thus MIL-53(Fe) preferentially adsorbs up to 50 wt% S/N heterocycles that can act as H-bond acceptors; these completely replace the solvent that may initially fill the pores. Conversely the H-bond donor heterocycles are not capable of opening the structure and are not adsorbed. The breathing of the structure therefore plays a key role in the discrimination between BT and IND.

2.2 Separation of isomeric mixtures

As structural isomers or stereoisomers have similar boiling or melting points or crystallisation properties, the separation of isomeric mixtures is one of the most difficult challenges in industry.[2] For many applications it is of paramount importance to have pure isomeric forms, as impure mixtures can be unreactive, toxic or lead to inferior derived products.[52] Adsorptive separation of isomers with zeolites is already an established technology for several complex mixtures.[1,3,53] However, there is still room for improvement, especially for enantiomeric separations as chiral zeolites are exceedingly rare and difficult to make.

Separation of structural isomers. An industrially relevant example of a complex mixture containing structural isomers is that of ethylbenzene (EB) and *m*/*o*/*p*-xylene (*m*/*o*/*p*X), which often also contains benzene (B) and toluene (T) (BTEX-mixture). Although each of these compounds can be processed into valuable compounds, *p*X is of considerable importance in the large scale synthesis of polyester polymers (*e.g.* polyethylene terephthalate). Due to the very close proximity of the boiling points of *p*X (138 °C), *m*X (138–139 °C) and EB (136 °C), the industrial separation of the xylene isomers is conducted either by a crystallisation process or by adsorption on zeolites.[2] Improving the separation factors between the isomers is not trivial using zeolites. As MOFs possess a higher degree of tailorability because of the almost infinite number of possible metal–ligand combinations, they offer potential to improve these separation factors. Moreover, the lower density of MOFs compared to zeolites should increase the uptake capacity on a weight basis significantly. The first MOFs that were successfully used for the separation of xylene isomers were MIL-47, MIL-53(Al) and HKUST-1.[54] The competitive adsorption equilibria of liquid mixtures of two C8 alkylaromatic compounds in hexane showed that HKUST-1 could only discriminate significantly between *m*X and *o*X, having a separation factor of 2.4. By contrast, MIL-53(Al) and MIL-47 could discriminate between several isomers and for both materials the high preference of *p*X over EB was remarkable. MIL-47 also preferred *p*X over *m*X, while MIL-53(Al) was only marginally effective to discriminate between these two isomers. Breakthrough experiments with diluted xylene isomer mixtures in hexane using a MIL-47 packed column gave average selectivities of 2.5 for the separation of *p*X *versus* *m*X and 7.6 for the separation of *p*X *versus* EB. A full regeneration of the column was possible by flushing with hexane. In order to understand this remarkable preference for the *p*X molecules, Rietveld refinements of the X-ray powder diffraction patterns of MIL-47 samples saturated with each of the aromatic compounds were performed. The refinements showed that the *p*X molecules fill the channels of MIL-47 in a pairwise fashion with close π–π interactions between the *p*X molecules (Fig. 6). These observations led to the conclusion that the selectivity arises from a molecular packing effect, rather than from interaction of the isomers with the framework constituents themselves.

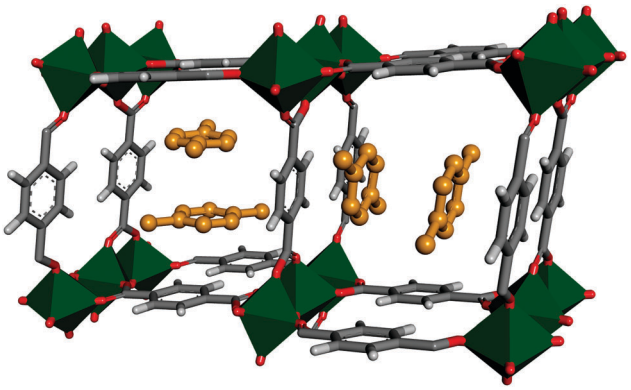

Fig. 6 Pairwise stacking of *p*X (orange) in MIL-47(V) as determined by Rietveld refinement (V: green; O: red; C: gray; H: white).

Following these results, the effect of the activation process of MIL-47 on the selectivity for *p*X and *m*X separation was assessed.[55] The optimal calcination time at 573 K was 21.5 h, at which all residual terephthalate molecules are removed from the pores and the BET surface area reaches a maximum value of 750 $m^2\ g^{-1}$. The fully activated material was evaluated as an adsorbent for other disubstituted aromatic isomers. Irrespective of the functional group, MIL-47 has a pronounced preference for the *para*-substituted xylene, ethyltoluene, dichlorobenzene, toluidine and cresol over the *meta*- and *ortho*-substituted isomers. For xylene and dichlorobenzene the efficient molecular packing of the isomers seems to be the reason for the high selectivity for the *para*-substituted isomer. However, for the ethyltoluene, toluidine and cresol isomers, the molecular packing is not found to be decisive, but rather the formation of specific lattice-adsorbate hydrogen bonds is an important factor determining selectivity for the cresol and toluidine isomers.

Although MIL-47 is selective for *p*X over *m*X, it does not discriminate between *p*X and *o*X. In view of these findings, a computational screening of different topologies was employed.[57] On the basis of simulation data, which were confirmed by experimental verification, MIL-125(Ti)–NH_2, MIL-125(Ti) and CAU-1(Al)–NH_2 were found to be capable of selectively adsorbing *p*X out of a mixture of xylenes. All these MOFs have the same **fcu**-topology built up of cyclic $(Ti/Al)_{12}O_8(OH)_4(COO)_{12}$ octamers linked by BDC or 2-aminoterephthalates. Breakthrough experiments with binary solutions of xylenes in heptane using a column filled with MIL-125(Ti)–NH_2 allowed the calculation of average separation factors of 2.2 for *p*X *versus* *o*X and 3.0 for the important couple *p*X/*m*X; these values corresponded well to the separation factors obtained from the molecular simulations. The pronounced *para*-selectivity is attributed to a more efficient molecular packing of *p*X molecules in both the octahedral and

tetrahedral cages, thereby maximizing adsorbate–adsorbate as well as adsorbate–framework interactions in comparison with *o*X and *m*X isomers. Moreover, the *para*-selectivity of the MIL-125 topology was further confirmed with alkylaromatics having shapes and kinetic diameters comparable to those of xylenes. MIL-125(Ti)–NH_2 selectively adsorbed the *para*-isomers of ethyltoluenes and cymenes, thereby proving not only the shape selectivity of the material, but also its broad applicability.

In a follow-up study, the influence of ethylbenzene on the *para*-selectivity of MIL-125(Ti)–NH_2 was investigated with ternary and quaternary breakthrough experiments in *n*-heptane as eluent.[58] These experiments confirmed that MIL-125(Ti)–NH_2 is a *para*-selective material as *p*X is the most retained isomer, even in the presence of *m*X and *o*X isomers. However, the *para*-selectivity decreased from 2.7 to 1.1 when the concentration of xylene isomers increased. When EB was present in the feed, the selectivity of *p*X/EB dropped to 1.4 at low concentration and even inversed to 0.8 at higher xylene concentrations. These observations showed that MIL-125(Ti)–NH_2 becomes EB selective at high feed concentrations due to a very efficient stacking of the EB molecules in the octahedral cages of the structure.

In a search for MOF materials with different xylene isomer preferences (Table 3), the flexible MIL-53(Al) was investigated by Alaerts *et al.*[56] Besides xylene, also cymene and ethyltoluene isomer mixtures were investigated by means of batch, pulse chromatographic and breakthrough adsorption experiments. In competitive batch experiments using binary solutions of xylenes in hexane, MIL-53(Al) appeared to be *o*X selective, with a strikingly high *o*X/EB selectivity of 10.9. This high *ortho*-selectivity was further confirmed in breakthrough experiments, with average selectivities of 11.0 for *o*X over EB and 2.2 for *o*X over *m*X. When single compound adsorption isotherms were recorded, a peculiar inversion in preference was observed for *p*X and *m*X as the curve of *p*X crosses the curve of *m*X: at low concentrations MIL-53(Al) prefers *m*X, while at higher concentrations more *p*X is adsorbed. The overall *ortho*-selectivity for ternary mixtures is also observed for larger molecules such as ethyltoluene and cymene isomers. It was concluded that the structure is markedly *ortho*-selective, even though the molecular size of ethyltoluene and cymene is substantially larger than that of xylene. In order to understand this *ortho*-preference, the authors performed Rietveld refinements on the xylene/ethyltoluene/cymene loaded samples (Fig. 7). Upon adsorption of *o*X, the obtuse angle β between opposing terephthalate ligands is reduced from 104.9° for an empty MIL-53(Al) structure to 97.8°, which is a stronger deformation of the channels compared to the effects induced by adsorbed *meta*- or *para*-isomers, with β-values of 98.2° and 100.8° respectively. This deformation is due to the simultaneous interaction of both methyl groups of *o*X with the carboxylate groups of the framework, while *m*X and *p*X molecules can only interact with the carboxylate groups *via* one methyl group. The refinements of the cymene and ethyltoluene loaded structures revealed similar distortions and interactions with the framework (Fig. 7).

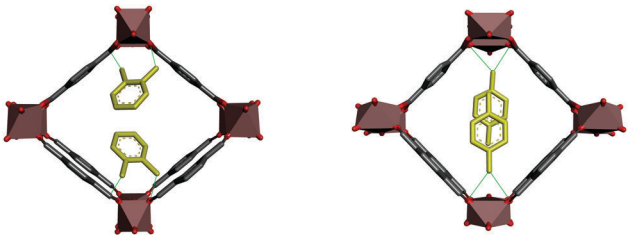

Fig. 7 Adsorption of *o*X (left) and *p*X (right) in MIL-53(Al) as determined by Rietveld refinements. *o*X interacts with the framework through both methyl groups (green), while *p*X only interacts with one methyl group. This causes a stronger reduction of β in the case of *o*X.

Inspired by the strong *ortho*-selectivity of the MIL-53(Al) structure, a study was conducted for finding the appropriate eluent for using this material in industrial process conditions.[61] The group of Rodrigues used single and multicomponent pulse liquid chromatographic experiments to measure selectivities for xylene mixtures with isooctane, *n*-hexane and *n*-heptane as eluents. Very low selectivities are obtained with isooctane as solvent, while the *ortho*-preference is clearly observed for *n*-hexane and *n*-heptane. The combination of the calculated selectivities and the observed retention times makes *n*-heptane the most appropriate solvent, as it is easily displaced by the xylene isomers. Breakthrough experiments with the three different solvents further confirmed the *ortho*-selectivity of the material and demonstrated that the eluent plays an important role in xylene separation. The same group evaluated the pelletized form of MIL-53(Al) in a pilot scale unit and obtained an *o*X selectivity of 2.0 over *m*X and *p*X and a xylene saturation capacity of 6.76 mol kg^{-1}.[62] As this mass based capacity is three times higher than that of the *state-of-the-art* adsorbents, this material shows great potential for the complete separation of *o*X from the other xylene isomers.

The analogous MIL-53(Fe) structure displays a distinctly different breathing behaviour compared to the Al analogue and was therefore used in a detailed study of the separation of the BTEX-mixture.[59] Single compound adsorption isotherms showed a clear preference for *o*X with uptakes up to 40 wt%, while *p*X and *m*X only reached uptakes of 25 wt%. It is important to note that the isotherms for *p*X and *m*X display several steps indicative of breathing behaviour, while no steps are present for *o*X. Rietveld refinements reveal that even though the stacking of *o*X and *m*X is quite similar, the interactions of *m*X with the structure are much weaker compared to the interactions of *o*X with the structure. For *p*X the interactions are

Table 3 Overview of MOFs applied in xylene separations

		Separation factor α						
MOF	Solvent	*o*X/*p*X	*o*X/*m*X	*p*X/*m*X	*p*X/EB	*o*X/EB	*m*X/EB	Ref.
HKUST-1	Hexane	0.7	0.4	0.9	1.2	0.7	1.4	54
MIL-53(Al)	Hexane	3.5	2.7	0.8	3.1	10.9	3.8	54, 56
MIL-47	Hexane	1.4	2.0	2.9	9.7	10.9	4.2	54
MIL-125(Ti)–NH_2	Heptane	0.45	1.0	3.0	1.4	—	—	57, 58
MIL-53(Fe)	Heptane	3.5	1.3	0.38	3.5	12.3	9.2	59
UiO-66	Heptane	2.4	1.8	—	—	—	—	60

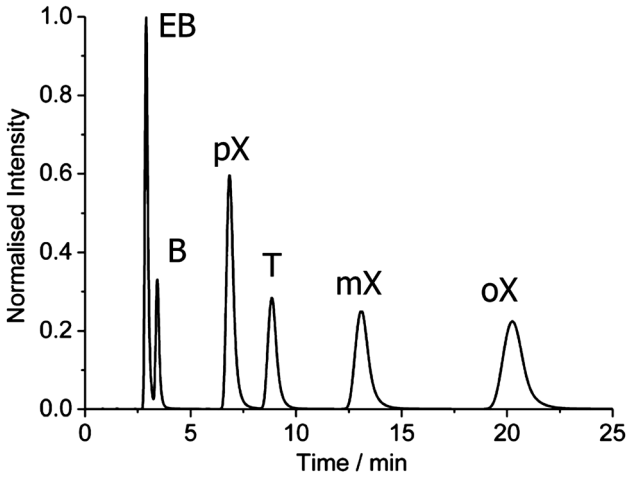

Fig. 8 Pulse chromatogram of BTEX on a MIL-53(Fe) column at 323 K with the following order of elution: ethylbenzene (EB), benzene (B), *para*-xylene (*p*X), toluene (T), *meta*-xylene (*m*X) and *ortho*-xylene (*o*X).[59]

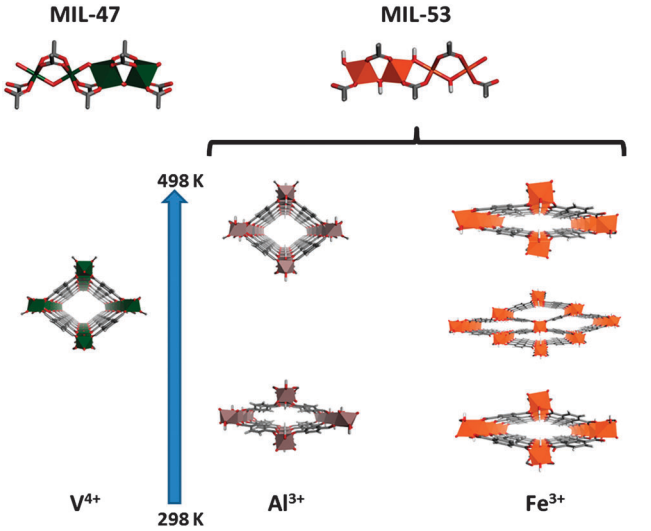

Fig. 9 Differences in chemistry and breathing behaviour between MIL-47(V) and MIL-53(Al/Fe). MIL-47 (left) shows no breathing and lacks μ_2-OH groups due to the 4+ oxidation state of V (green). MIL-53 materials display temperature- and guest-dependent breathing, which is significantly impacted by the metal. For Al (center; purple), the framework switches between a closed (low T) and an open (high T) phase. In MIL-53(Fe) (right) switching between the low temperature hydrous form and the high temperature anhydrous form proceeds *via* an intermediately anhydrous framework with two distinct channel types[63] (O: red; C: gray; H: white; Fe: orange).

even weaker due to the zigzag arrangement of *p*X molecules in the pores of MIL-53(Fe). In any case, the complete separation of the individual compounds of the BTEX mixture is possible with MIL-53(Fe) at 323 K, as proven by pulse chromatographic experiments (Fig. 8).

The order of xylene elution is *para*, followed by *meta* and then *ortho*. This is in contrast to the related materials MIL-47(V), which has a preference for *p*X, and MIL-53(Al), which shows poor discrimination between *para* and *meta* isomers.[54,56] Despite having similar structures, MIL-47, MIL-53(Al) and MIL-53(Fe) display very different separation performances (Table 3) due to the different chemistry in all three materials: the oxidation states of the metals are different (4+ for V and 3+ for Al and Fe); MIL-47 has no hydroxyl groups lining the pores as opposed to MIL-53(Al) and MIL-53(Fe); and the breathing behaviour of all three materials is significantly different (Fig. 9).

Another material with *ortho*-selectivity similar to MIL-53(Al) is the Zr-terephthalate UiO-66, either in powder or in pelletized form.[60] This framework is constructed from $Zr_6O_4(OH)_4$ SBUs which are twelve-fold connected through terephthalates in a face-centered cubic lattice. UiO-66 presents a selectivity pattern that is the reverse of that of the xylenes' molecular dimensions with respect to shape selectivity. Breakthrough experiments with *n*-heptane as the mobile phase indicated that there is a 42% loss in capacity but only a slight loss in selectivity when pelletized UiO-66 is used compared to the powder form. The selectivities of *o*X over *m*X and *p*X are 1.7 and 2.3 in the pelletized form and 1.8 and 2.4 in the powder form. This selectivity behaviour of UiO-66, which is based on entropic effects in the small tetrahedral cages,[64] makes it a suitable material for *o*X isolation from *n*-heptane in the extract ('heavy' product) or *p*X isolation in the raffinate ('light' product) by simulated moving bed technology.

The remarkable separation power of UiO-66 was also exploited for the liquid phase separation of cyclic isomers, namely functionalized cyclohexane derivatives.[65] In the case of 4-ethylcyclohexanol, a clear preference was noticed for the *cis* isomer, which is in perfect agreement with previously performed gas phase separations of dimethylcyclohexanes.[66] The *cis*/*trans* selectivity could be further increased by reducing the ratio of methanol/acetonitrile in the mobile phase. A similar trend was observed for *cis*/*trans*-3-methylcyclohexanol, where the separation factor increased by decreasing the fraction of methanol in the mobile phase. The reason for this interesting separation capability is most likely an interplay between entropic effects produced by confinement in the smallest cages and enthalpic effects due to the presence of the OH group which enhances the interaction between the isomers and the framework.

The alkylation of benzene with propylene leads to the formation of a mixture of two isomers: cumene as the major compound, together with traces of *n*-propylbenzene. The separation of these alkylaromatics was studied in detail with the vanadium terephthalate MIL-47.[67] Both competitive batch adsorption and liquid phase pulse chromatography experiments revealed a strong preference of MIL-47 for *n*-propylbenzene over cumene with an average separation factor of 2.2 for the pulse chromatographic experiments. Using the van't Hoff plot, the authors were able to calculate the apparent adsorption enthalpies of *n*-propylbenzene and cumene as −12.4 and −5.9 kJ mol^{-1}. The linear side chain of *n*-propylbenzene is able to interact better through hydrogen atoms of the sp^3 hybridized carbon atoms with the carboxylate groups of the structure than the branched side chain of cumene. This explains the lower observed apparent adsorption enthalpy. The authors extended the investigation of apparent adsorption enthalpies to alkylbenzenes with alkyl chains of increasing length, such as ethylbenzene

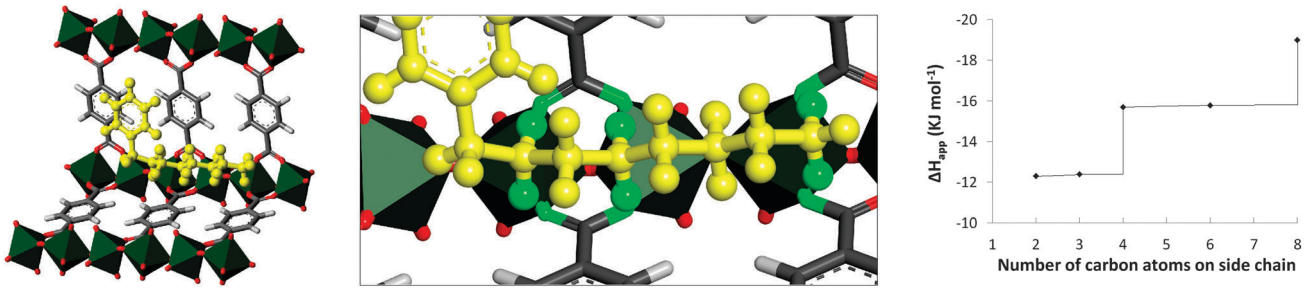

Fig. 10 Adsorption of alkylaromatics in MIL-47. The apparent adsorption enthalpy increases stepwise with the length of the alkyl chain due to an increasing number of hydrogen bonding contacts with the framework carboxylates. For *n*-octylbenzene (yellow), such interaction (green) can occur three times (V: gray octahedra; O: red; C: gray; H: white).

(−12.3 kJ mol^{-1}), *n*-propylbenzene (−12.4 kJ mol^{-1}), *n*-butylbenzene (−15.7 kJ mol^{-1}), *n*-hexylbenzene (−15.8 kJ mol^{-1}) and *n*-octylbenzene (−19.0 kJ mol^{-1}) (Fig. 10, left). The stepwise increase of the apparent adsorption enthalpy (Fig. 10, right), with −3.2 kJ mol^{-1} increments, is in perfect agreement with the number of –(CH_2)– segments that are able to interact with the framework carboxylates, *viz.* 1 for alkyl side chain lengths of C_2–C_3, 2 for chain lengths of C_4–C_7, and 3 for a C_8 chain length (Fig. 10, middle).

The same authors explored the fractionation of the petrochemical naphthalene fraction with [Cu_2(BDC)$_2$(DABCO)] (DABCO = 1,4-diazabicyclo[2.2.2]octane, BDC = 1,4-benzenedicarboxylic acid), a compound from the family of structures widely explored by Kitagawa and his group.[68–70] This framework consists of two-dimensional layers of Cu–terephthalate paddlewheel complexes, connected into a three-dimensional structure using DABCO as a pillaring ligand. The adsorption isotherms of the isomers 1-methylnaphthalene and 2-methylnaphthalene diluted in heptane both levelled off at 25 wt%, corresponding to 1 molecule per unit cell. The unsubstituted naphthalene and disubstituted 1,4-dimethylnaphthalene are substantially less adsorbed, with 13 and 6 wt% respectively. This suggests that the methyl substituent has an important interaction with the framework, leading to higher loadings compared to the unsubstituted naphthalene. For the disubstituted 1,4-dimethylnaphthalene the authors deduced that the additional methyl substituent may prevent uptake due to size restrictions. Even though single compound adsorption isotherms show similar uptakes for both monomethylnaphthalene isomers, competitive adsorption experiments in heptane showed a preferential uptake of 1-methylnaphthalene over 2-methylnaphthalene with a separation factor of 2.6 at high loadings. This separation factor increased with the concentration of the isomers, which is indicative of packing effects, with the 1-methylnaphthalene being packed more efficiently. Further competitive experiments with [Cu_2(BDC)$_2$(DABCO)] not only showed the possibility to discriminate between 1-methylnaphthalene and 2-methylnaphthalene, but also the ability to separate these monomethylnaphthalenes from other naphthalene compounds in the fraction.

For the fractionation of reactive heteroaromatic isomers, Dong and co-workers explored the separation power of a Cd–triazolate framework [$Cd(L)_2(ClO_4)_2$] (L = 4-amino-3,5-bis(4-pyridyl-3-phenyl)-1,2,4-triazole).[71] When crystals of this MOF were immersed in mixtures of 2-furaldehyde and 3-furaldehyde, or of 2-thiophenaldehyde and 3-thiophenaldehyde, only the 2-substituted isomers were adsorbed, as confirmed by ^{1}H-NMR. This high selectivity was attributed to the polar nature of the pore walls, created by the aminosubstituted triazole moieties of the ligand and the ClO_4^- anions, together with the shape of the pores. In the case of toluidine isomers, the selectivity is toward the *ortho*-substituted isomer, most likely due to the more polar nature of the *ortho*-toluidine (*ortho*-toluidine = 1.61 Debye; *meta*-toluidine = 1.49 Debye; *para*-toluidine = 1.36 Debye).[72] The adsorbent could be easily regenerated by washing with acetonitrile.

MIL-100(Fe) is also able to separate toluidine and chloroaniline isomers in normal-phase HPLC separations, *i.e.* using a predominantly polar solid phase and a less polar eluent.[73] The separation of these isomers was greatly affected by the solvent composition of the mobile phase. By increasing the methanol content of the dichloromethane/methanol mobile phase, the retention times of the isomers were greatly reduced. A baseline separation of the toluidine and chloroaniline isomers was possible with a volumetric dichloromethane/methanol ratio of 99.3/0.7. The *ortho*-isomer eluted before the *meta*- and *para*-isomers, for both toluidine and chloroaniline. The authors linked the separation mechanism to the electron density on the nitrogen atom in the adsorbates, which increases as the pK_b of the compounds decreases. A larger electron density on the nitrogen atom in the *para*-isomer leads to a stronger interaction with the CUS sites in MIL-100(Fe) and such compounds are therefore retained most strongly. The effect of temperature on selectivity was also investigated and the analysis of the van't Hoff plot confirmed a separation mechanism based on enthalpic effects, as the separation factor between the isomers decreased with increasing temperature.[67]

Even though aliphatic hydrocarbon isomers are important for industry, especially considering the upgrading of petroleum or other feedstocks by separating the branched compounds from the linear ones, the use of MOFs for separating these compounds in the liquid phase has hardly been explored. In one of the few studies, MIL-96(Al), an aluminium 1,3,5-benzenetricarboxylate featuring both chains and μ_3-O bridged

trimers of Al-octahedra, was used for the separation of some C5-hydrocarbons, with a focus on the dienes isoprene, *trans*-piperylene and *cis*-piperylene.[74] Single compound adsorption isotherms of these three compounds were recorded using *n*-heptane as a solvent. The structure showed a remarkable preference for *trans*-piperylene over isoprene and *cis*-piperylene, due to steric constraints generated by the cages of the MIL-96(Al) structure, preventing the uptake of more than 1 molecule of isoprene or *cis*-piperylene per cage. A more efficient packing of the *trans*-piperylene therefore explains the higher uptake of this compound. Breakthrough experiments with a packed MIL-96(Al) column showed an average separation factor of 3.1 for *trans*-piperylene over isoprene. MIL-96(Al) was not able to discriminate between *cis*-piperylene and isoprene. The breakthrough profiles of *cis*-piperylene and isoprene show a striking feature, namely the crossing of both curves during the elution of the compounds. The authors attributed this effect to a difference in the diffusion rate of these compounds when passing through the adsorbent bed. The much larger time interval needed for isoprene to reach a full breakthrough compared to *cis*-piperylene indicates a significantly slower diffusion through the cages of the structure due to the branched nature of this C5 diene molecule.

The group of Kitagawa explored the use of core–shell functionalized crystals of $Zn_2(BDC)_2(DABCO)$ for the extraction of branched paraffins.[75] They fabricated core–shell heterostructures in which the storage container is the core crystal based on 1,4-benzenedicarboxylate and the size separation filter is the shell crystal with 9,10-anthracene dicarboxylate as the linker (Fig. 11). Individual functionalised and unfunctionalised crystals were immersed for a week in solutions of *n*-cetane, iso-cetane and a mixture of *n*/iso-cetane, followed by an investigation with microscopic laser Raman spectroscopy (MLRS). The Raman spectra show that the functionalised crystals were only able to adsorb the linear *n*-cetane, while the unfunctionalised crystals were not able to discriminate between the cetane isomers. The uptake of *n*-cetane from a pure *n*/iso-cetane mixture was estimated at 26.9 wt% with a 100% selectivity for the linear isomer, making this a promising shape-selective approach for separation of branched isomers from their linear counterparts.

A final example of an adsorbent for the selective adsorption of stereoisomers is the cobalt–porphyrintetracarboxylate PIZA-1 which features trinuclear Co^{2+} carboxylate clusters which connect to eight Co^{3+}-functionalized porphyrin rings.[76] Channels of 9 Å × 7 Å and 14 Å × 7 Å are present in the framework, creating a void volume of 74%. Size-, shape- and functional group-selective sorption indicated a marked preference for polar molecules like water, amines and alcohols. Besides good solvent drying capabilities, the structure showed excellent shape-selective sorption behaviour for substituted alkylamines. The linear alkylamines were taken up three times more compared to substituted isomers. This shape-selective adsorption was attributed to the more difficult interaction of the sterically more hindered di-butylamines. The importance of the interaction of the functional group with the structure was further proven by comparing the adsorption of 1/2-propanol and 1/*t*-butanol. The uptake of the branched alcohols was significantly lower compared to that of the linear isomers.

Enantiomers. As many biologically active compounds are chiral, obtaining pure enantiomeric compounds is important in both pharmaceutical and agrochemical industries. The development of chiral adsorbents therefore potentially creates an important new tool for these industries. Due to the synthesis of MOFs under relatively mild conditions, the fabrication of a homochiral framework is more feasible for MOFs than for conventional zeolites, where chirality is often lost during calcination of the framework, and which contain hardly any functional groups that could serve as docking points in chiral recognition.[77] Although the synthesis of a homochiral MOF is relatively easy, the use of these frameworks in chiral separations in the liquid phase is rather limited so far.[78]

The first example of enantioselective adsorption in liquid phase conditions was given by Seo *et al.* with the homochiral framework D-POST-1, which features a $Zn_3(\mu_3\text{-}O)$ SBU similar to that of MIL-100 and MIL-101. Each Zn^{2+} is coordinated to one μ_3-O, and to four carboxylate oxygen atoms and a pyridyl nitrogen from the chiral D-tartaric acid-derived linker (Fig. 12a).[79] This robust enantiopure metal–organic cluster builds up a framework with large 1D channels. When the structure was exposed to a racemic methanol solution of the chiral $[Ru(2,2'\text{-bipyridine})_3]Cl_2$ complex, an enantiomeric excess (ee) of 66% was achieved as confirmed by NMR, UV-VIS spectroscopy and circular dichroism measurements. These results established that homochiral MOFs can be successfully applied for the separation of racemic mixtures. A similar strategy was used for quitenine (Fig. 12b) (QA) to generate a $Cd(QA)_2$ MOF with a **dia**-topology.[80] The adamantine type cavities were able to enantioselectively adsorb small organic molecules, such as 2-butanol and 2-methyl-1-butanol. The material and the racemic compounds were mixed under

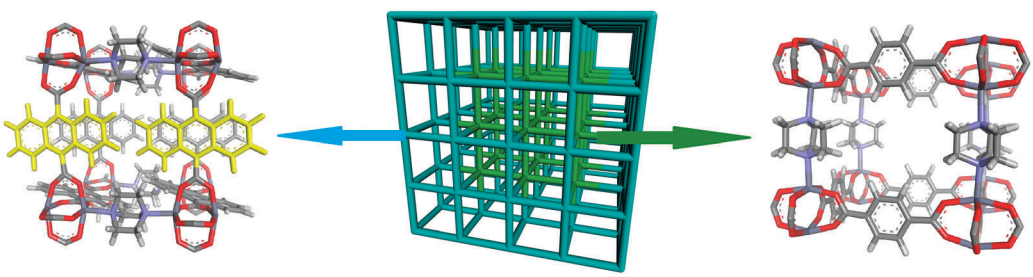

Fig. 11 Core–shell functionalized particles of $Zn_2(BDC)(DABCO)$. The outer shell (blue) is functionalized with 9,10-anthracenedicarboxylate linkers (yellow), while the core (green) consists of BDC linkers (Zn: dark blue; O: red; N: blue; C: gray; H: white).

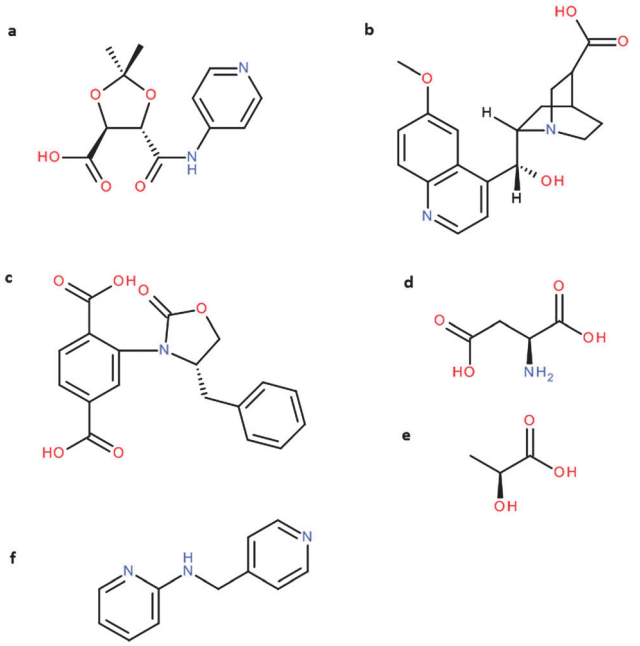

Fig. 12 Chiral linkers used for the construction of enantioselective MOFs. (a) D-POST-1: (4*S*,5*S*)-2,2-dimethyl-5-[(4-pyridinylamino)carbonyl]-1,3-dioxolane-4-carboxylic acid; (b) Cd(QA)$_2$: 6-methoxy-(8*S*,9*R*)-cinchonan-9-ol-3-carboxylic acid; (c) Bn-ChirUMCM-1: (*S*)-2-(4-benzyl-2-oxooxazolidin-3-yl)terephthalic acid; (d) L-aspartic acid; (e) L-lactic acid; (f) *N*,*N*′-(2-pyridyl)-(4-pyridylmethyl)amine.

solvothermal conditions and investigated with single-crystal X-ray diffraction. The structural analysis showed an ee of 98.2% and 8.3 wt% adsorption of the (*S*)-2-butanol, *versus* an ee value of only 8.2% for the larger (*S*)-2-methyl-1-butanol. This striking difference in selectivity for molecules of different size immediately exposes a potential weakness of chiral MOF adsorbents, namely that a small size misfit of the adsorbates can lead to a dramatic lowering of the enantioselectivity.

The combination of three-connected 3D nets and the small templating 1,2-propanediol offers an alternative mechanism for inducing chirality in MOFs, as the topology of such frameworks is often chiral due to the presence of helices in the extended structures.[81] This approach was used for the synthesis of the chiral $Ni_3(BTC)_2(PIC)_6(1,2\text{-}PD)_3$ framework (PIC = picoline, 1,2-PD = 1,2-propanediol), where (*R*)-1,2-propanediol gave exclusively right-handed helices in this 2-fold interpenetrating (10,3)-a net topology. A remarkable dependency of enantioselectivity on adsorbate size was observed for menthone, fenchone and binaphthol (Fig. 13). While menthone and fenchone are too small compared to the pore dimensions to obtain enantioselectivity, a modest ee of 8.3% is achieved for the larger binaphthol. The authors concluded that a close match between pore dimensions and adsorbate size is required for selective adsorption of one of the enantiomers.

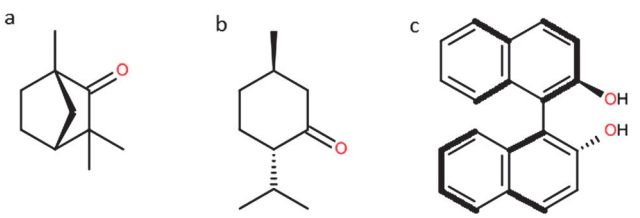

Fig. 13 Fenchone (a), menthone (b) and *R*-binaphthol (c).

One of the first successful column experiments with chiral MOFs was performed by the group of Kaskel.[82] The ligand 2-bromoterephthalic acid was modified with (*S*)-oxazolidinone to obtain a chiral BDC linker (Fig. 12c), which was used to synthesize the Zn material Bn-ChirUMCM-1 or $Zn_4O(BTB)_{4/3}$-(Bn-ChirBDC)$(DEF)_{20}(H_2O)_8$. The incorporation of the chiral auxiliary (4*S*)-benzyl-2-oxazolidinone into the structure was proven with $^{13}C\{^1H\}$ cross-polarization MAS-NMR. The spectra revealed a thermal rotational motion of the chiral group inside the pores of the structure. Chromatographic experiments showed that the material was capable of separating racemic 2-butanol and 1-phenylethanol solutions, with the (*R*)-isomers being the most retained compounds. The strongest interaction with the chiral selector was observed for the 1-phenylethanol, having a separation factor for (*R*/*S*) of 1.6. However, tailing of the peaks resulted in a rather low resolution of 0.65, due to unoptimized gradient elution and column length.

Another straightforward choice as chiral building blocks for homochiral MOFs is naturally occurring compounds like amino acids, as they are cheap and readily available. This approach was used for the construction of an aspartic acid (Fig. 12d) based MOF with enantioselective adsorption properties.[83] The structure is built up by Ni-(L-aspartate) layers linked together by 4,4′-bipyridine, forming 1D channels of 3.8 Å × 4.7 Å. The authors did note that the solvent composition of the synthesis mixture has to be carefully controlled to avoid racemization of the amino acid at higher temperatures. The adsorption of several chiral diols, with enantiomer excesses varying from 3.4% ee for 2,5-hexanediol up to 54% ee for 2-methyl-2,4-pentanediol, was studied and some crucial insights needed for successful enantioselective separations were derived. Even though some diols have similar chain lengths, the position of the hydroxyl groups on the carbon backbone is the determining factor for the quality of the separation. With the combination of experimental adsorption and computational calculations for 1,2-pentanediol and 2-methyl-2,4-pentanediol, the factors responsible for enantioselection were investigated. As expected based on the exactly identical lengths of the carbon backbones, the calculations revealed similar adsorption sites inside the chiral pockets of the structure. However, only the secondary alcohol group of (*S*)-1,2-pentanediol interacts with the framework through hydrogen bonding with a carboxylate group of an aspartate and the amine group of another aspartate, while both hydroxyl groups of (*S*)-2-methyl-2,4-pentanediol are involved in hydrogen bonding within the chiral pocket, resulting in a higher enantiomer excess (Fig. 14). This observation led the authors to conclude that the size of the chiral pocket has to match well the molecular size of the adsorbates in combination with the right chemical environment in order to realize enantioselective separations.

L-Lactic acid (Fig. 12e) is another cheap naturally occurring molecule that is produced by a simple fermentation process; it was

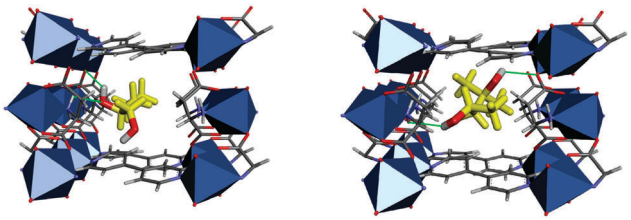

Fig. 14 Adsorption of (*S*)-1,2-pentanediol (left, yellow) and (*S*)-2-methyl-2,4-pentanediol (right, yellow) in the chiral pocket of Ni_2(L-asp)$_2$(bipyridine). (*S*)-1,2-Pentanediol only interacts through hydrogen bonds (green) with one OH-group, whereas (*S*)-2-methyl-2,4-pentanediol can interact with both hydroxyl groups, leading to a higher ee for this compound (Ni: blue polyhedra; N: light blue; O: red; C: gray; H: white).

used for the synthesis of the homochiral [Zn_2(BDC)(L-LAC)(DMF)] framework (DMF = *N*,*N*-dimethylformamide).[84,85] The chiral center of the L-lactate ligand is exposed to the 1D pores, providing the structure with a chiral environment close to the Zn-oxo chains. In the initial study, the uptake of several substituted sulfoxides from dichloromethane was investigated.[84] The sulfoxides with smaller substituents, including methylsulfonylbenzene and 1-bromo-4-(methylsulfonyl)benzene, were adsorbed up to 23 and 7 wt% respectively. The ee values were found to be 20% for methylsulfonylbenzene and 27% for 1-bromo-4-(methylsulfonyl)benzene, thus showing the potential of this framework for enantioselective liquid phase adsorption. In a follow-up study, the same authors prepared a HPLC column of the Zn-lactate material in order to study the preparative chromatographic separation of racemic sulfoxides in dichloromethane in more detail.[85] The chromatograms indicated that only methylsulfonylbenzene was nicely separated with good resolution; a separation factor of 4.5 and an enantiomer excess of 60% were achieved. The incomplete separation of NO_2- and Br-substituted sulfoxides was attributed to the electron withdrawing substituents which prevent a strong coordination within the framework. It was suggested that electron donating groups could provide a stronger interaction with the framework, but steric hindrance of an additional methyl or isopropyl group will lead to slower internal diffusion, resulting in decreased enantioselectivity.[78]

In a different approach, chirally discriminating MOFs can also be synthesised with cheap achiral building blocks. One of the first MOFs showing enantioselective intercalation using only achiral building units is [Cu(PPh$_3$)(*N*,*N*′-(2-pyridyl-(4-pyridylmethyl)-amine))$_{1.5}$]·ClO_4 (Fig. 12f).[86] The structure crystallizes in the chiral space group *R*3 and is able to enantioselectively intercalate racemic 2-butanol. The enantiopure 2-butanol could be obtained by physically separating the different homochirally loaded crystals and subsequently evacuating the crystals, even if this may not offer a solution for practical use. In a similar synthesis approach the homochiral Co_2(INA)$_4$(H_2O) (INA = isonicotinate) was crystallized using only achiral building blocks.[87] This MOF is constructed from Co_2(μ_2-H_2O)(INA)$_8$ SBUs which are bound in an **ecu**-topology featuring Co_2(μ_2-H_2O)(μ_2-INA) helices interconnected by INA linkers. The presence of two different helical substructures leads to two enantiomorphous single crystal phases, as confirmed by solid state circular dichroism measurements. It is clear that single crystals from the conglomerate of Co(INA)$_2$, constructed from either right-handed or left-handed helices, can effectively separate organic racemates. Co(INA)$_2$ with right-handed helices selectively adsorbed only (*S*)-2-butanol, (*R*)-styrene oxide and (*R*)-1-phenylethanol out of the racemic mixtures. Structure analysis of single crystals loaded with 1-phenylethanol indicated specific hydrogen bonding interaction as the mechanism underlying the enantioselective uptake. The enantiopure compounds could easily be extracted from the single crystals without modifying the uptake capacity. However, in both these studies the presence of two enantiomorphous phases makes the separation of chiral compounds on a large scale a time consuming process due to the need for physical separation of the individual crystallites before enantiopure compounds can be extracted.

2.3 Molecules with different size and functionality

The adsorption and separation of chemical compounds differentiated by size and/or functional groups will be discussed in the following paragraphs. Due to the infinite number of combinations of organic ligands with inorganic units, MOFs can be designed for the selective adsorption of functional molecules by modifying the pore size, the exposed functional groups or even by changing the nature of the open metal sites. Due to the ease of modification of MOFs, they are an excellent choice for the separation of these mixtures.

A nice example of selective adsorption based on differences in functional groups was reported by Xu *et al.*[88] In this study the selective adsorption of some C6–C8 aromatic compounds was reported for the manganese MIL-53 analogue Mn_2(BDC)$_2$(BPNO)$_4$, with BPNO = 4,4′-bipyridine-*N*,*N*′-dioxide. In this framework, the inorganic chains are built up of Mn(O_{BDC})$_4$(μ_2-O_{BPNO})$_2$-octahedra, as the O-atoms of BPNO replace the μ_2-OH groups in MIL-53. This results in the connection of adjacent chains by BPNO as well as by BDC linkers. When soaking the evacuated crystals of this flexible material in pure solutions of benzene, toluene, chlorobenzene, ethylbenzene and *p*/*m*/*o*-xylene, single crystal analysis of the exchanged crystals showed that only benzene, toluene and chlorobenzene were intercalated in the structure. The selective uptake of these three compounds was investigated in binary competitive adsorption experiments. A selectivity trend of chlorobenzene > benzene > toluene was recorded. This was attributed to the different degree of π–π interactions and possible H-bonding mechanisms. While toluene can only interact with one phenyl ring of the pore wall due to the additional methyl group, benzene and chlorobenzene can engage in multiple interactions simultaneously. Additionally, the higher selectivity for chlorobenzene over benzene was attributed to possible Cl···H–C bonding with the framework.

This inspired a different group to evaluate UiO-66, MIL-125(Ti)(NH_2), HKUST-1 and MIL-101(Cr) for the liquid phase adsorption of chloroaromatic compounds.[89] The single compound adsorption equilibria of chlorobenzene, 2-chlorotoluene, 1,3-dichlorobenzene, and 2-chloroanisole over the prepared MOFs were measured in batch mode using 1,3,5-triisopropylbenzene as a solvent. At the highest tested concentration

MIL-101(Cr) had the largest uptake capacity (>40 wt%) for all evaluated compounds, while MIL-125(Ti)–NH_2 had the highest affinity for these chloroaromatic compounds at low concentrations. This high affinity was attributed to the hydrogen bonding interaction of the amino groups with the chloroaromatics. The capacity of MIL-125(Ti)–NH_2 and MIL-101(Cr) was found to be superior to that of activated carbon. When mixtures of chloroaromatic compounds were presented to both MOFs, chloroanisole was the preferred compound irrespective of the concentration range.

Also for $Zn_2(BTC)(NO_3)$ a selective uptake of molecules out of the liquid phase based on interaction of specific functional groups with the structure was observed.[90] In this MOF two Zn atoms are coordinated by three carboxylate groups, two oxygen atoms of a bidentate NO_3^- and three ethanol molecules resulting in a trigonal bipyramidal configuration of the zinc atoms. These SBUs are linked by hexadentate BTC linkers. After ethanol removal, the structure has 1.4 nm hexagonal channels and three CUS per two Zn atoms, which can bind molecules through coordination with the open metal site. Adsorption experiments with solutions containing 1% of single compounds in toluene showed that the structure can take up alcohols like methanol, ethanol, and *t*-butyl alcohol, but not the sterically hindered *t*-butylphenol or nonalcoholic molecules such as chloroform, 1,2-dichloroethane, acetonitrile and methyl ethyl ketone. This indicates that there is a selectivity mechanism based on the functional group, with a clear preference for interaction of sterically non-hindered alcohols with the unsaturated metal sites. When expanding the adsorption experiments to alcohol mixtures with C1 to C7, the overall order of alcohol selectivity by this material is C1, C2 > C3, C4 > C5, C7, which is in qualitative agreement with that expected on the basis of a shape- and size-selective inclusion process.

Another example of the separation of molecules with different functional groups is a recent study by Fu *et al.*[73] MIL-100(Fe) was used as a stationary phase in a HPLC column for the reversed phase separation of two groups of analytes: the neutral aromatics benzene, toluene, ethylbenzene, naphthalene, and 1-chloronaphthalene; and the basic compounds aniline, acetanilide, 2-nitroaniline, and 1-naphthylamine. The chromatogram for the neutral compounds with methanol/H_2O as the mobile phase follows the elution order (Fig. 15, left) benzene > toluene > ethylbenzene > naphthalene > 1-chloronaphthalene. The retention of these compounds was severely affected by the composition of the mobile phase, and this was related to the hydrophobicity of the analytes. The best resolution was obtained with 43% methanol, while at 100% the analytes eluted simultaneously after the dead volume and 0% methanol led to very long retention times and poor resolution.

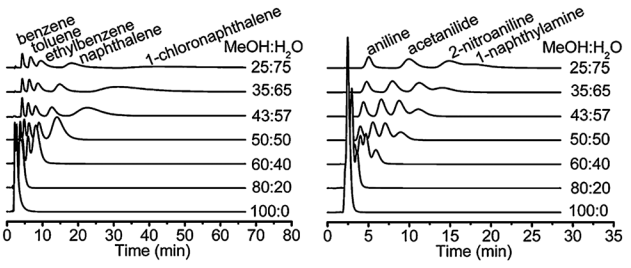

Fig. 15 Effect of the mobile phase composition on the HPLC separation on a MIL-100(Fe) packed column (5 cm long × 4.6 mm i.d.): (left) benzene, toluene, ethylbenzene, naphthalene and 1-chloronaphthalene (5 μL, 0.01 mol L^{-1} each); (right) aniline, acetanilide, 2-nitroaniline and 1-naphthylamine (5 μL, 0.01 mol L^{-1} each).[73]

For the basic compounds the elution is based on a combination of steric constraints and basicity following the order of (Fig. 15, right) aniline > acetanilide > 2-nitroaniline > 1-naphthylamine. The composition of the mobile phase had a similar effect on the elution of the compounds as was observed when increasing the methanol content in the binary methanol/H_2O mobile phase for the neutral compounds. A decreasing methanol content increased the retention of the compounds. For both the neutral and basic analytes the retention was increased with longer alkyl chain lengths and the number of aromatic rings. The authors suggested a strong π–π interaction as the main reason for the strong retention of the naphthyl compounds. Additionally, the influence of temperature on the retention of the compounds was studied in the temperature range of 298–348 K. By constructing van't Hoff plots, apparent adsorption enthalpies were calculated. The compounds that were retained the strongest, naphthylamine and 1-chloronaphthalene, had the highest apparent adsorption enthalpies. The performance of the MIL-100(Fe) column was further investigated by attempting multiple chromatographic cycles, which showed an excellent reproducibility of the separations, making this material a promising stationary phase for normal phase HPLC analysis.

The separation of saturated *versus* unsaturated molecules can be achieved with MOFs by relying on different separation mechanisms. The potential of the CUS of HKUST-1 was explored for the important separation of ethylbenzene and styrene.[91] This separation is very energy-intensive due to similar boiling points of both compounds, resulting in substantial efforts in the search for alternative separation methods. HPLC experiments with an HKUST-1 column as the stationary phase showed a successful separation with styrene being the most retained compound. The separation is proposed to be due to the coordinative interaction of styrene with the CUS of copper in the stationary phase, *i.e.*, a π-complexation mechanism. However, due to the large difference in the particle size of the HKUST-1 crystallites, the use of such a polydisperse mixture as an HPLC stationary phase inevitably leads to undesirable peak shapes (Fig. 16A) and high column backpressures (up to 200 bar), as confirmed by Ameloot *et al.*[92] Therefore, HKUST-1 was directly synthesized inside the pores of monodisperse silica spheres typically used as an HPLC stationary phase, combining the good column packing properties of the silica with the separation ability of the MOF material. Without the MOF crystallites inside the pores, the silica particles were not able to separate ethylbenzene and styrene (Fig. 16B), while the silica–MOF composite material was found to separate mixtures of ethylbenzene and styrene effectively under the same conditions, with retention times of 4 and 12 min, respectively (Fig. 16C).[92]

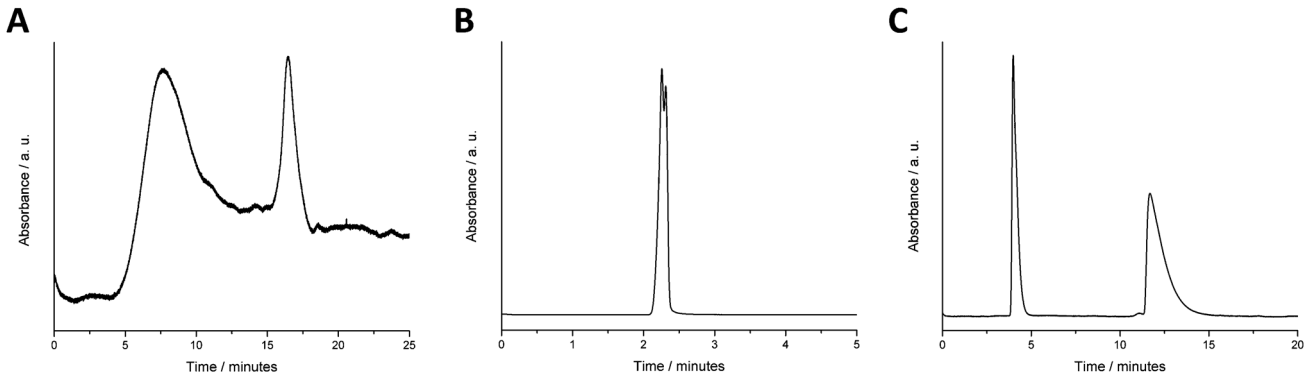

Fig. 16 Separation of a mixture of ethylbenzene and styrene on a pure HKUST-1 column (A). Separation of the same mixture on an unmodified silica column (B). Separation of the same mixture on a silica column modified with HKUST-1 (C).[92]

Inspired by these results, the separation of several unsaturated alkylaromatics, including styrene, from their saturated analogues was investigated with HKUST-1.[93] A breakthrough experiment of styrene and ethylbenzene from heptane on a HKUST-1 column showed a clear preference for styrene accompanied by a roll-up effect, indicating that the less preferred ethylbenzene is displaced by the more strongly adsorbing styrene. The average separation factor was calculated to be 2. The interaction of styrene and ethylbenzene with the CUS of HKUST-1 was confirmed with UV-VIS spectroscopy by a shift in d–d transitions. As both compounds appear to be interacting through their π-electrons with the CUS, the preferential adsorption of styrene is mainly governed by the total number of π-electrons present in the adsorbate. Also for ethyltoluene (ET) and vinyltoluene (VT), both for the *para*- and the *meta*-substituted isomers, the structure preferentially adsorbed the VTs over the ETs. The separation factors for the competitive batch adsorption experiments were *ca.* 6.5 for *p*VT *versus p*ET and 2.6 for *m*VT *versus m*ET. This difference in the separation factor between the isomers was attributed to steric hindrance imposed by the methyl substituent in the *meta* position.

However, the use of CUS for the separation of ethylbenzene and styrene is not mandatory, as evidenced with MIL-53(Al) and MIL-47.[94] The potential of these two MOFs with similar structures for the separation of ethylbenzene and styrene containing feeds was explored in detail. Their structures were previously described in detail (Fig. 9); MIL-53(Al) has a hydrophilic pore structure exhibiting breathing behaviour, while MIL-47 has hydrophobic pores and is more rigid. Competitive adsorption experiments out of heptane showed that both materials selectively adsorb styrene over ethylbenzene, with a saturation level of 20 wt% for styrene and a separation factor around 3.5–4 in static conditions. Column breakthrough experiments confirmed the selectivity of both materials for styrene with average separation factors of 2.9 and 2.3 for MIL-47 and MIL-53(Al) respectively. The adsorption mechanism was further probed by temperature dependent pulse-chromatographic experiments. For MIL-47 the separation factor of approximately 5 was independent of the temperature in the 298–348 K range. This suggests that the adsorption enthalpies of both compounds must be quite similar in MIL-47, as the relative retention of the compounds is dependent on the ratio of adsorption equilibrium constants and this ratio remained constant in the investigated temperature range. By using the van't Hoff equation, apparent adsorption enthalpies of -9.0 kJ mol^{-1} for ethylbenzene and -10.1 kJ mol^{-1} for styrene were calculated. As both apparent adsorption enthalpies are quite similar, the adsorption preference must be based on entropic differences. Rietveld refinement confirmed that in a tripled unit cell, ethylbenzene can occupy only two of its 12 possible adsorption positions in the presence of styrene, while styrene molecules can be accommodated on all of their 8 possible positions inside the pores (Fig. 17). This implies a much larger number of possible adsorbate arrangements for styrene, and hence a higher entropy than for ethylbenzene. The latter therefore loses more freedom in the transition from the surrounding liquid to

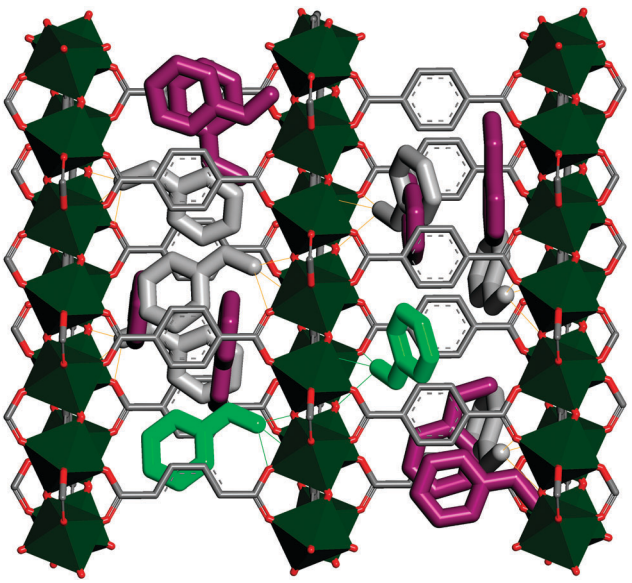

Fig. 17 Stacking of ethylbenzene in styrene-loaded MIL-47. Styrene (purple) is packed pairwise in the channels of MIL-47, occupying several adsorption sites of ethylbenzene (gray). Only two of the possible adsorption sites for ethylbenzene are occupied (green).[94]

the adsorbed state in the pores, while the adsorption enthalpy is similar for both components. The adsorption mechanism for MIL-53(Al) is different. While the separation factor for styrene over ethylbenzene at 298 K is 3.9, the value decreased to 2.3 at 348 K, showing a clear temperature dependence, which indicates a difference in adsorption enthalpy; ethylbenzene has an apparent adsorption enthalpy of -13.1 kJ mol^{-1} while the adsorption enthalpy of styrene is much more negative at -24.2 kJ mol^{-1}. Also for MIL-53(Al), Rietveld refinement confirmed that the deformation of the O–Al–O angles is less pronounced when styrene is adsorbed compared to the adsorption of ethylbenzene, which results in a more negative adsorption enthalpy for styrene. In spite of MIL-47 and MIL-53(Al) being structural analogues, the separation of styrene and ethylbenzene is based on a very different mechanism: MIL-47 displays a unique packing of styrene molecules based on differences in entropy, while in MIL-53 enthalpic effects play a key role.

3. Aqueous phase

3.1 Low concentrations of organics in water

In order to probe the potential of MOFs for the adsorptive removal of pharmaceuticals from water, the stability towards hydrolysis[95,96] of several frameworks was investigated by studying the effect of water concentration on a diverse set of structures with different metal clusters and organic linkers.[97] The structures used in this study were MOF-177, MOF-5, HKUST-1, MOF-505, UMCM-150, ZIF-8 and MIL-100(Cr). The stability of the frameworks was investigated by analysing the powder diffraction patterns of the materials exposed to various concentrations of water in DMF. Only MIL-100(Cr) and ZIF-8 were found to be stable in pure water during a period of one week. The stability of MIL-100(Cr) was attributed to the strength of the Cr_3–μ_3-oxo cluster, while for ZIF-8 the high pK_a of the 2-methylimidazolate results in a very stable metal–ligand bond. Soaking both materials for 12 months in water showed that only MIL-100(Cr) was absolutely stable, while ZIF-8 was only kinetically stable in water as structural changes appeared after 3 months. Therefore, the adsorption capacity for two pharmaceuticals, furosemide and sulfasalazine (Fig. 18), was evaluated for MIL-100(Cr) at very low concentrations. It exhibited an excellent performance with a furosemide uptake capacity of 1.2 wt% at a concentration of 7.50 μg mL^{-1} water and a sulfasalazine uptake capacity of 0.6 wt% at a concentration of 1.40 μg mL^{-1}. In comparison, the adsorption of both pharmaceuticals on NaY zeolite did not result in any significant uptake due to strong coadsorption of water molecules inside the zeolite.

One of the first studies to explore the adsorption of organic compounds from an aqueous solution with MOFs was performed by Bai *et al.*[98] The framework in this study consisted of Cu_6S_6 clusters linked by triazine-containing ligands and had luminescent properties associated with the Cu-cluster. The authors used this luminescent property to detect organic contaminants usually found in wastewater. They discovered that the adsorption of toluene, nitrobenzene, aniline and *p*/*m*/*o*-xylene from 0.5% aqueous solutions effectively quenched the luminescence due to π–π and hydrogen bonding interactions. The uptake of toluene from a 0.5% aqueous solution was measured with thermogravimetric analysis (TGA) to be 8 wt%. Thereby, the authors not only achieved the detection of several aromatics in aqueous solutions, but demonstrated the potential of MOFs for the adsorption of organic molecules out of aqueous solutions.

In view of the high chemical stability of the MIL-101(Cr) framework,[99] the removal of benzene from a 1000 ppm aqueous solution was studied in batch adsorption experiments with MIL-101(Cr) and activated carbon.[100] MIL-101(Cr) combined a higher adsorption capacity (80 wt% at saturation) and affinity with faster adsorption kinetics compared to the activated carbon (45 wt% at saturation). These properties were attributed to the combination of a very large surface area with a small particle size of the MOF crystallites, resulting in a superior adsorbent. Considering these results it is not surprising that MIL-101(Cr) was further studied for the removal of organics from water in several other studies.[101–103]

The removal of methyl orange (Fig. 19a) from wastewater was evaluated with two Cr MOFs, MIL-101(Cr) and MIL-53(Cr).[103] The open metal sites of MIL-101(Cr) were post-synthetically grafted with ethylenediamine (MIL-101(Cr)-ED) and protonated ethylenediamine (MIL-101(Cr)-PED). The adsorption kinetics were tested for different concentrations and compared with active carbon (granule, 2–3 mm). The adsorption time needed for reaching adsorbent saturation follows the order activated carbon > MIL-53(Cr) > MIL-101(Cr) > MIL-101(Cr)-ED > MIL-101(Cr)-PED, and a fair agreement was found with a pseudo-second-order kinetic model for all adsorbents. The capacity of the adsorbents followed the same trend as the

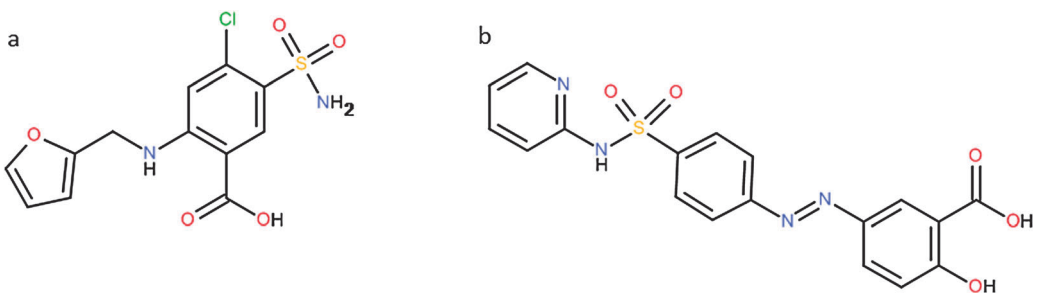

Fig. 18 Furosemide (a) and sulfasalazine (b).

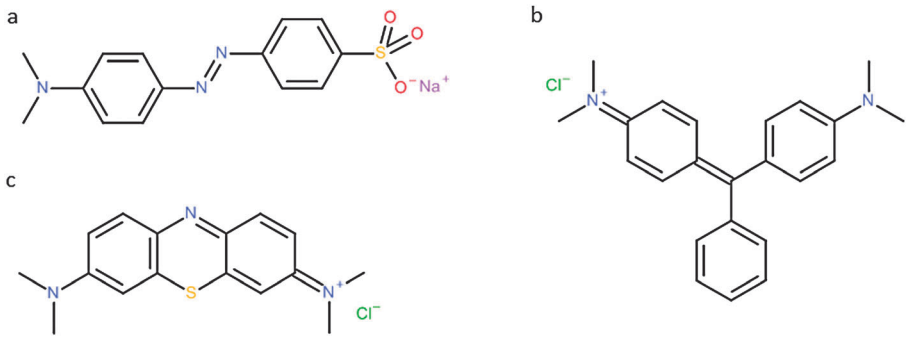

Fig. 19 Dyes adsorbed from aqueous solutions with MOFs: methyl orange (a); malachite green (b) and methylene blue (c).

kinetics: activated carbon < MIL-53(Cr) < MIL-101(Cr) < MIL-101(Cr)-ED < MIL-101(Cr)-PED. The modified MIL-101(Cr) samples combine fast kinetics with high adsorption capacities, at 17.5 wt% uptake for MIL-101(Cr)-PED and 12.5 wt% for MIL-101(Cr)-ED. The apparent adsorption enthalpy obtained from the van't Hoff plot for MIL-101(Cr)-PED is 29.5 kJ mol^{-1}. The regeneration of the adsorbent by washing with water followed by ultrasound treatment was successful and did not affect the capacity.

Also for the removal of a nonsteroidal anti-inflammatory drug (naproxen) and a bioactive metabolite (clofibric acid) (Fig. 20), MIL-101(Cr) was found to be a superior adsorbent compared to MIL-100(Fe) and active carbon.[101] Both MIL-100(Fe) and MIL-101(Cr) reached adsorption equilibrium after 2 h, while for active carbon a contact time of at least 6 h was required to reach adsorption equilibrium. A relation was established between the adsorption capacities and the Langmuir surface area. Variation of the pH (4–12) showed a decrease in uptake capacity with increasing pH. With naproxen having a pK_a of ~4, an electrostatic interaction was proposed between the positively charged MIL-101(Cr) and the anionic naproxen. The decrease in capacity at higher pH is explained by a diminished positive charge of the framework at higher pH, leading to weaker interactions.

This high naproxen uptake from aqueous solutions inspired others to employ a MIL-101(Cr) microcolumn for online adsorptive extraction and direct analysis of naproxen and its metabolites from urine samples.[102] First, the uptake of naproxen from aqueous solutions was evaluated for a multi-walled carbon nanotube (MWCNT), a C18 bonded silica and MIL-101(Cr). MIL-101(Cr) had the highest uptake in the tested concentration range (6.0 wt%), followed by the MWCNT (2.5 wt%) and the C18 bonded silica (2.4 wt%). The high uptake on MIL-101(Cr) was further analysed at different temperatures, revealing an increased uptake at higher temperatures, indicative of an endothermic adsorption process. In order to evaluate the performance of MIL-101(Cr) for the extraction of naproxen from urine samples, the material was packed into a microcolumn and parameters including pH of the sample solution, sample flow rate, sample volume, desorption solvent and time were investigated in detail and optimized. This allowed the calculation of the enrichment factor of naproxen and its metabolite 6-*O*-desmethylnaproxen, 290 and 295 respectively, by comparing the sensitivity before and after online enrichment.

Besides Cr-based MOF materials, stable Fe–μ_3-oxo based MOFs were tested to adsorb contaminants, for example malachite green (Fig. 19b), from polluted aqueous environments. The adsorbents included MIL-100(Fe), MIL-53(Al), MIL-101(Cr) and activated carbon.[104] MIL-100(Fe) was found to be a superior adsorbent compared to the other tested materials, reaching a 25 wt% uptake of malachite green from an aqueous solution at pH 5. As the stability and the ionization of malachite green (pK_a 10.3) may be affected by the pH of the solution, the adsorption capacity of MIL-100(Fe) was evaluated at different pHs (Fig. 21). The adsorption capacity of MIL-100(Fe) for malachite green increased as the pH increased from 1 to 4,

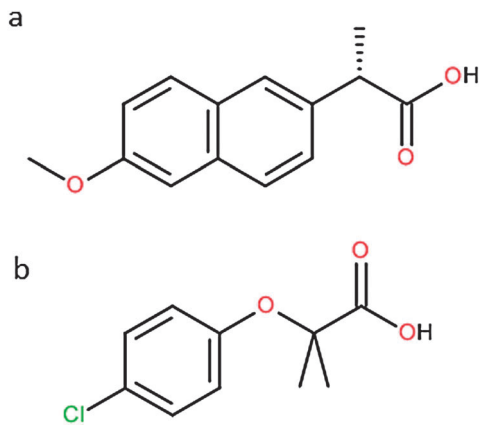

Fig. 20 Naproxen (a) and clofibric acid (b).

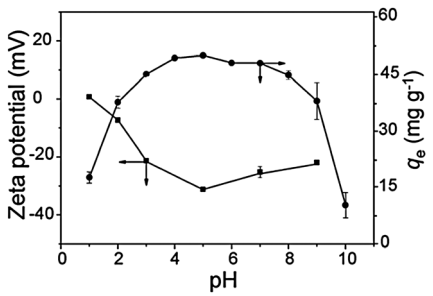

Fig. 21 The ζ-potential of MIL-100(Fe) (left vertical axis) and the amount of malachite green adsorption (right vertical axis) as a function of pH.[104]

then levelled off in the pH range of 4 to 7, and decreased with the further increase of pH from 7 to 10. This is explained by the more negative zeta potential of the MOF particles upon increasing the pH from 1 to 5, which is favourable for the adsorption of the positively charged malachite green. In the higher pH range of 8–10, the malachite green is increasingly deprotonated, leading to a diminished uptake at higher pH. The use of X-ray photoelectron spectroscopy (XPS) revealed that the adsorption of malachite green led to a shift of the N1s peak of the malachite green to higher energy and a shift to lower energy for the Fe 2p peak in MIL-100(Fe). This was interpreted as an electrostatic interaction of the nitrogen heteroatom in malachite green with the metal sites in MIL-100(Fe), thereby displacing water molecules bound to the open metal site. The adsorbed malachite green could be easily removed by washing the adsorbent with 0.5 wt% HCl in ethanol solution.

Similarly, the adsorption of the cationic dye methylene blue (Fig. 19c) and the anionic dye methyl orange (Fig. 19a) was investigated with MOF-235. MOF-235, $[Fe_3O(BDC)_3(DMF)_3][FeCl_4]$, is constructed, similarly as MIL-88, by μ_3-oxo clusters of Fe, linked together by terephthalates and coordinated DMF molecules. This results in a positively charged framework, which is balanced by one $[FeCl_4]^-$ anion per unit formula. Logically, the affinity of this positively charged framework for the anionic methyl orange is much higher than that for the positive methylene blue.

Maes *et al.* reported the use of a flexible material, MIL-53(Cr), for the adsorption of phenolics and sugars from water.[105] The performance of this breathing and water-stable framework was compared with active carbon as a benchmark material for the removal of phenolics from wastewater. Single compound adsorption isotherms show a higher uptake capacity of phenol and *p*-cresol for MIL-53(Cr) compared to active carbon, with 14 volume% of phenol and *p*-cresol on MIL-53(Cr) and 10 volume% for both compounds on active carbon. Even though both materials have similar pore volumes of approximately 0.5 ml g^{-1}, their difference in density (0.4 g cm^3 for MIL-53 *versus* 0.32 g cm^3 for activated carbon) results in a volumetric capacity that is 40% higher for MIL-53(Cr) compared to active carbon. As the affinity for an adsorbent in the removal of contaminants from water is especially important, the adsorption at very low concentrations was further investigated. MIL-53(Cr) still outperformed active carbon at an equilibrium concentration of 0.015 M phenol with 3.4 volume% uptake for MIL-53(Cr) compared to 2.0 volume% uptake for active carbon. When studying the adsorption isotherm of phenol on MIL-53(Cr) in more detail, a clear step was observed around 5 volume% uptake. This was identified as the opening of the structure when the threshold concentration of phenol was reached. Finally, breakthrough experiments were performed using a 0.02 M aqueous phenol solution and a 0.5 g MIL-53(Cr) column. The curve of phenol on MIL-53(Cr) showed again a stepwise profile, whereby initially all phenol is retained on the column. After elution of a limited volume of pure water, phenol started to break through. Once the framework is in a more opened conformation, more phenol is adsorbed, resulting in a second breakthrough at a larger eluted volume (Fig. 22). In addition, the authors probed the MIL-53(Cr) column for its capacity to isolate sugars out of an aqueous solution. The column experiment confirmed that the material is able to adsorb the small sugar D-fructose.

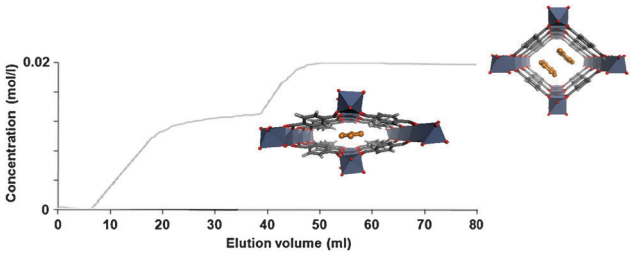

Fig. 22 Breakthrough adsorption of phenol (0.02 M in water) over a 5 g MIL-53(Cr) column. The stepwise profile is attributed to the opening of the framework upon adsorption of phenol, allowing for additional phenol molecules (orange) to be stacked in the channels.[105]

3.2 Separations of bio-based chemicals

One of the main challenges in the production of bio-based chemicals is their recovery from the aqueous phase.[27] Distillation is not always a suitable approach in the case of chemicals from renewable resources due to the reactive nature of many compounds. However adsorption could be a valid alternative for specific cases as it is typically carried out at lower (ambient) temperature. As the potential of MOFs for aqueous phase separations has only recently been tapped, only a few studies have focussed on this area, but it can be expected that a significant increase in research interest in this area will be seen in the next years.

Until now, only the recovery of bio-butanol and furfural has been evaluated with MOFs, more specifically with ZIF-8.[106–108] Furfural is regarded as an important platform molecule in future biorefineries as it can be derived from lignocellulose. For low furfural concentrations in aqueous product streams (*e.g.*, <3 wt%), recovery using traditional techniques is not desirable.[107] Therefore, a homogeneous ZIF-8-silicone rubber nanocomposite membrane was used for pervaporation of furfural from a liquid aqueous feed. The membrane contained a high particle loading and was supported on a hierarchically ordered stainless-steel mesh. Not only a high selectivity factor between furfural and water is required, but also a sufficiently high flux through the membrane is necessary for industrial implementation. Single compound adsorption isotherms of furfural and water on ZIF-8 powders show a clear preference for furfural, with 45 wt% adsorption at saturation and nearly no adsorption of water. This corresponds to six furfural molecules per ZIF-8 cage. The permeability and selectivity of the composite membrane were evaluated at 80 °C for different feed concentrations. An almost constant selectivity factor of 10 and a permeability of 10^4 Barrer for furfural were achieved at different feed concentrations (0.5–3 wt%). Upon increasing the operating temperature (60–120 °C), both the furfural permeability and the selectivity decreased due to a diminished furfural adsorption in the membrane. This performance exhibits a high potential for integrating a membrane unit with a furfural stream stripper to realize continuous biorefining.

Bio-butanol is a promising alternative for petroleum based fuels as it has a higher energy density and lower volatility compared to bio-ethanol. The production occurs through the

fermentation of biomass, from which the selective recovery from a low concentrated solution is the main bottleneck. Because ethanol and acetone are major side products in the fermentative production of bio-butanol, the adsorption and separation of lower 1-alcohols, acetone, and water on ZIF-8 were studied. Vapour phase adsorption isotherms of the alcohols have a sigmoidal shape, with very low adsorption at low partial pressure due to the hydrophobic nature of the material. The pressure at which adsorption starts decreases with increasing alcohol chain length. It was established that a structural transition is needed for ZIF-8 to accommodate the 1-butanol. Twisting of the imidazolate linkers results in an increase of the size of the narrow windows which link the nanocages throughout the framework, thereby providing sufficient space for butanol to enter the cages of the structure (Fig. 23). The liquid phase adsorption isotherms of methanol, ethanol, propanol, and butanol dissolved in *tert*-butanol as a non-adsorbing solvent also showed sigmoidal shapes. However, when the alcohols were dissolved in water, the step in the isotherm occurred at much lower concentrations. A competitive adsorption experiment with butanol, ethanol and acetone from water showed that butanol is the most preferred compound with an uptake around 30 wt%. Powder diffraction analysis of ZIF-8 crystals loaded with butanol revealed no additional twisting of the imidazole linkers. The Rietveld refinement suggests that six butanol molecules are adsorbed per cage, corresponding to 28 wt% adsorption. On the other hand, acetone, ethanol and water are not adsorbed by ZIF-8.

Following these results, the same group developed a conceptual adsorption process with a combination of adsorbents for the recovery and purification of bio-butanol.[108] In the first stage the adsorption of butanol from the fermentation medium containing side products like acetone and ethanol takes place on ZIF-8. This is followed by purification of the butanol enriched phase by removing water, ethanol and acetone.[106] Selectivities calculated from breakthrough experiments on ZIF-8 are 10.2 and 2.6 for 1-butanol over ethanol and acetone respectively. In order to evaluate the effect of residual salts, acids, sugars or metabolites in the aqueous fermentation solution, adsorption in the presence of these traces was investigated to validate ZIF-8 as a potential adsorbent. The capacity and selectivity of ZIF-8 for butanol were not affected by any of these compounds. After the upconcentration of butanol, traces of ethanol, acetone and water could be removed by adsorptive separation on the zeolite SAPO-34. This allowed removal of smaller primary alcohols and water molecules from the concentrated butanol solution. Therefore, it can be concluded that the combination of the MOF ZIF-8 and the zeolite SAPO-34 is a very attractive solution for the recovery and purification of bio-butanol by adsorption.

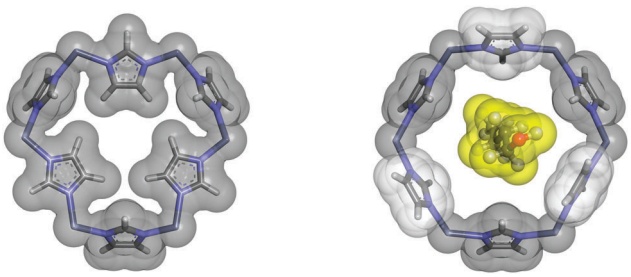

Fig. 23 Flipping of the imidazolate groups of the "closed" window in ZIF-8 (left) allows for 1-butanol to enter through the now open window (right) and to be adsorbed in the cages.

4. Conclusions and perspectives

Since their discovery, metal–organic frameworks have grown from novelty porous materials to full-fledged adsorbents capable of competing with state-of-the-art adsorbent materials. Not only have MOFs shown to be superior to more traditional materials in separating xylenes or in desulfurizing fuels, but also previously inaccessible selectivities have come within reach thanks to their unique host–guest interactions. The combination of inorganic metal nodes connected by organic linkers creates a chemically diverse environment inside MOF pores which allows specific interactions between adsorbates and both the organic and inorganic parts of the framework. A good understanding of these interactions and the underlying mechanisms will allow future researchers not only to exploit and improve the separation power of known frameworks, but also to design new MOFs based on these acquired insights. Major progress can still be anticipated in chiral separations as only a minority of the available chiral frameworks have been tested. While initial studies focused mainly on the separation of mixtures from hydrocarbon streams, the discovery of more stable frameworks in recent years opened the door to separations from aqueous media as well. It was illustrated that MOFs can have great potential in both the removal of dyes and pharmaceuticals from water and the recovery of biobased chemicals from aqueous streams. As new stable MOFs are being synthesized continuously, more possibilities will become available for aqueous phase separations, which will be increasingly important in a future bio-based industry. It is therefore recommended that future researchers should focus more on investigating aqueous, bio-based mixtures. Hence, scientific breakthroughs in the field of liquid phase adsorptive separations can be anticipated with water-stable materials. Studying chiral separations on enantiopure MOFs remains another highly topical field of research, with potential applications in chiral chromatography, even if fair comparison with the currently available chiral chromatography columns should be made.

Abbreviations

1,2DMI	1,2-Dimethylindole
1,2-PD	1,2-Propanediol
2MI	2-Methylindole
AMSA	Aminomethanesulfonic acid
B	Benzene
BDC	1,4-Benzenedicarboxylate
BPNO	4,4′-Bipyridine-*N*,*N*′-dioxide
BT	Benzothiophene
BTB	1,3,5-Benzenetribenzoate
BTC	1,3,5-Benzenetricarboxylate
BTEX	A mixture of toluene, ethylbenzene and xylene isomers

BTZ	Benzothiazole
CBZ	Carbazole
CUS	Coordinatively unsaturated sites
DABCO	1,4-Diazabicyclo[2.2.2]octane
DBT	Dibenzothiophene
DEF	*N*,*N*-Diethylformamide
DMDBT	4,6-Dimethyldibenzothiophene
DMF	*N*,*N*-Dimethylformamide
EB	Ethylbenzene
ED	Ethylenediamine
EDXRD	Energy-dispersive X-ray diffraction
ee	Enantiomeric excess
ET	Ethyltoluene
GO	Graphene oxide
HDN	Hydrodenitrogenation
HDS	Hydrodesulfurization
HPLC	High performance liquid chromatography
INA	Isonicotinate
IND	Indole
IR	Infrared
L-asp	L-Aspartic acid
L-LAC	L-Lactic acid
MAS-NMR	Magic angle spinning nuclear magnetic resonance
MLRS	Microscopic laser Raman spectroscopy
MOF	Metal–organic framework
MWCNT	Multi-walled carbon nanotube
*m*X	*meta*-Xylene
NAPANA	6,6′,6″,6‴-((5′-(4-(Bis(6-carboxynaphthalen-2-yl)-amino)phenyl)-[1,1′:3′,1″-terphenyl]-4,4″-diyl)bis(azanetriyl))tetrakis(2-naphthoic acid)
NMC	*N*-Methylcarbazole
NMR	Nuclear magnetic resonance
*o*X	*ortho*-Xylene
PED	Protonated ethylene diamine
PIC	Picoline
PWA	Phosphotungstic acid
*p*X	*para*-Xylene
QA	Quitenine
QUI	Quinoline
SBU	Secondary building unit
T	Toluene
TGA	Thermogravimetric analysis
TIPB	Triisopropylbenzene
TP	Thiophene
UV-VIS	Ultraviolet-visible light
VT	Vinyltoluene
XPS	X-ray photoelectron spectroscopy

Acknowledgements

Both D.D.V. and J.D. are grateful to IWT (MOFShape). D.D.V. also thanks KULeuven for support through the Metusalem grant CASAS and IAP 7/05 Functional Supramolecular Systems. B.B. is grateful for a fellowship from FWO Vlaanderen.

References

1 R. T. Yang, *Adsorbents: Fundamentals and Applications*, 2007.
2 D. M. Ruthven, *Principles of adsorption and adsorption processes*, 1984.
3 S. Kulprathipanja, *Zeolites in Industrial Separation and Catalysis*, 2009.
4 C. R. Vitasari, G. W. Meindersma and A. B. de Haan, *Green Chem.*, 2012, **14**, 321.
5 J. F. Dechow, *Separation and Purification Techniques in Biotechnology*, Noyes Publications, 1989.
6 J.-R. Li, J. Sculley and H.-C. Zhou, *Chem. Rev.*, 2012, **112**, 869–932.
7 C. Moreno-Castilla, *Carbon*, 2004, **42**, 83–94.
8 E. C. De Oliveira, C. T. G. V. M. T. Pires and H. O. Pastore, *J. Braz. Chem. Soc.*, 2006, **17**, 16–29.
9 M. Hartmann and L. Kevan, *Chem. Rev.*, 1999, **99**, 635–664.
10 *Kirk-Othmer, Separation Technology*, John Wiley & Sons, Inc., Hoboken, NJ, 2nd edn, 2008.
11 V. A. Likholobov, V. B. Fenelonov, L. G. Okkel, O. V. Goncharova, L. B. Avdeeva, V. I. Zaikovskii, G. G. Kuvshinov, V. A. Semikolenov, V. K. Duplyakin, O. N. Baklanova and G. V. Plaksin, *React. Kinet. Catal. Lett.*, 1995, **54**, 381–411.
12 J. H. Cavka, S. Jakobsen, U. Olsbye, N. Guillou, C. Lamberti, S. Bordiga and K. P. Lillerud, *J. Am. Chem. Soc.*, 2008, **130**, 13850–13851.
13 K. S. Park, Z. Ni, A. P. Côté, J. Y. Choi, R. Huang, F. J. Uribe-Romo, H. K. Chae, M. O'Keeffe and O. M. Yaghi, *Proc. Natl. Acad. Sci. U. S. A.*, 2006, **103**, 10186–10191.
14 V. Colombo, S. Galli, H. J. Choi, G. D. Han, A. Maspero, G. Palmisano, N. Masciocchi and J. R. Long, *Chem. Sci.*, 2011, **2**, 1311.
15 K. Koh, A. G. Wong-Foy and A. J. Matzger, *J. Am. Chem. Soc.*, 2009, **131**, 4184–4185.
16 G. Férey, C. Mellot-Draznieks, C. Serre, F. Millange, J. Dutour, S. Surblé and I. Margiolaki, *Science*, 2005, **309**, 2040–2042.
17 W. J. Rieter, K. M. L. Taylor and W. Lin, *J. Am. Chem. Soc.*, 2007, **129**, 9852–9853.
18 K. K. Tanabe, Z. Wang and S. M. Cohen, *J. Am. Chem. Soc.*, 2008, **130**, 8508–8517.
19 T. Devic, P. Horcajada, C. Serre, F. Salles, G. Maurin, B. Moulin, D. Heurtaux, G. Clet, A. Vimont, J.-M. Grenèche, B. Le Ouay, F. Moreau, E. Magnier, Y. Filinchuk, J. Marrot, J.-C. Lavalley, M. Daturi and G. Férey, *J. Am. Chem. Soc.*, 2010, **132**, 1127–1136.
20 N. A. Ramsahye, T. K. Trung, S. Bourrelly, Q. Yang, T. Devic, G. Maurin, P. Horcajada, P. L. Llewellyn, P. Yot, C. Serre, Y. Filinchuk, F. Fajula, G. Férey and P. Trens, *J. Phys. Chem. C*, 2011, **115**, 18683–18695.
21 S. Kitagawa, R. Kitaura and S. Noro, *Angew. Chem., Int. Ed.*, 2004, **43**, 2334–2375.
22 D. Farrusseng, S. Aguado and C. Pinel, *Angew. Chem., Int. Ed.*, 2009, **48**, 7502–7513.
23 K. A. Cychosz, R. Ahmad and A. J. Matzger, *Chem. Sci.*, 2010, **1**, 293.

24 Z. R. Herm, E. D. Bloch and R. Long, *Chem. Mater.*, 2014, **26**, 323–338.
25 K. A. Cychosz and A. J. Matzger, *Langmuir*, 2010, **26**, 17198–17202.
26 S. K. Henninger, H. A. Habib and C. Janiak, *J. Am. Chem. Soc.*, 2009, **131**, 2776–2777.
27 H. D. Embree, T. Chen and G. F. Payne, *Chem. Eng. J.*, 2001, **84**, 133–147.
28 V. Chandra Srivastava, *RSC Adv.*, 2012, **2**, 759.
29 A. J. Hernández-Maldonado and R. T. Yang, *Catal. Rev.*, 2004, **46**, 111–150.
30 K. A. Cychosz, A. G. Wong-Foy and A. J. Matzger, *J. Am. Chem. Soc.*, 2008, **130**, 6938–6939.
31 K. A. Cychosz, A. G. Wong-Foy and A. J. Matzger, *J. Am. Chem. Soc.*, 2009, **131**, 14538–14543.
32 D. Peralta, G. Chaplais, A. Simon-Masseron, K. Barthelet and G. D. Pirngruber, *Energy Fuels*, 2012, **26**, 4953–4960.
33 S. Achmann, G. Hagen, M. Hämmerle, I. M. Malkowsky, C. Kiener and R. Moos, *Chem. Eng. Technol.*, 2010, **33**, 275–280.
34 G. Blanco-Brieva, J. M. Campos-Martin, S. M. Al-Zahrani and J. L. G. Fierro, *Fuel*, 2011, **90**, 190–197.
35 M. Maes, M. Trekels, M. Boulhout, S. Schouteden, F. Vermoortele, L. Alaerts, D. Heurtaux, Y.-K. Seo, Y. K. Hwang, J.-S. Chang, I. Beurroies, R. Denoyel, K. Temst, A. Vantomme, P. Horcajada, C. Serre and D. E. De Vos, *Angew. Chem., Int. Ed.*, 2011, **50**, 4210–4214.
36 S.-L. Li, Y.-Q. Lan, H. Sakurai and Q. Xu, *Chem.–Eur. J.*, 2012, **18**, 16302–16309.
37 N. A. Khan and S. H. Jhung, *J. Hazard. Mater.*, 2013, **260C**, 1050–1056.
38 B. Van de Voorde, A. S. Munn, N. Guillou, F. Millange, D. E. De Vos and R. I. Walton, *Phys. Chem. Chem. Phys.*, 2013, **15**, 8606–8615.
39 N. A. Khan and S. H. Jhung, *Angew. Chem., Int. Ed.*, 2012, **51**, 1198–1201.
40 B. Van de Voorde, M. Boulhout, F. Vermoortele, P. Horcajada, D. Cunha, J. S. Lee, J.-S. Chang, E. Gibson, M. Daturi, J.-C. Lavalley, A. Vimont, I. Beurroies and D. E. De Vos, *J. Am. Chem. Soc.*, 2013, **135**, 9849–9856.
41 A. L. Nuzhdin, K. A. Kovalenko, D. N. Dybtsev and G. A. Bukhtiyarova, *Mendeleev Commun.*, 2010, **20**, 57–58.
42 I. Ahmed, N. A. Khan, Z. Hasan and S. H. Jhung, *J. Hazard. Mater.*, 2013, **250–251**, 37–44.
43 I. Ahmed, Z. Hasan, N. A. Khan and S. H. Jhung, *Appl. Catal., B*, 2013, **129**, 123–129.
44 I. Ahmed, N. A. Khan and S. H. Jhung, *Inorg. Chem.*, 2013, **24**, 14155–14161.
45 F. Shi, M. Hammoud and L. T. Thompson, *Appl. Catal., B*, 2011, **103**, 261–265.
46 G. Blanco-Brieva, J. M. Campos-Martin, S. M. Al-Zahrani and J. L. G. Fierro, *Fuel*, 2013, **105**, 459–465.
47 G. Blanco-Brieva, J. M. Campos-Martin, S. M. Al-Zahrani and J. L. G. Fierro, *Fuel*, 2013, **113**, 216–220.
48 Z. Ismagilov, S. Yashnik, M. Kerzhentsev, V. Parmon, A. Bourane, F. M. Al-Shahrani, A. A. Hajji and O. R. Koseoglu, *Catal. Rev.*, 2011, **53**, 199–255.
49 Y. Yoshimura, M. Toba, H. Farag and K. Sakanishi, *Catal. Surv. Asia*, 2004, **8**, 47–60.
50 M. Macaud, M. Sévignon, A. Favre-Réguillon and M. Lemaire, *Ind. Eng. Chem. Res.*, 2004, **43**, 7843–7849.
51 E. A. van Nierop, S. Hormoz, K. Z. House and M. J. Aziz, *Energy Procedia*, 2011, **4**, 1783–1790.
52 L. A. Nguyen, H. He and C. Pham-Huy, *Int. J. Biomed. Sci.*, 2006, **2**, 85–100.
53 V. Cottier, J.-P. Bellat and M.-H. Simonet-Grange, *J. Phys. Chem. B*, 1997, **5647**, 4798–4802.
54 L. Alaerts, C. E. Kirschhock, M. Maes, M. van der Veen, V. Finsy, A. Depla, J. Martens, G. V. Baron, P. Jacobs, J. F. M. Denayer and D. E. De Vos, *Angew. Chem., Int. Ed.*, 2007, **46**, 4293–4297.
55 L. Alaerts, M. Maes, P. Jacobs, J. F. M. Denayer and D. E. De Vos, *Phys. Chem. Chem. Phys.*, 2008, **10**, 2979–2985.
56 L. Alaerts, M. Maes, L. Giebeler, P. A. Jacobs, J. A. Martens, J. F. M. Denayer, C. E. A. Kirschhock and D. E. De Vos, *J. Am. Chem. Soc.*, 2008, **130**, 14170–14178.
57 F. Vermoortele, M. Maes, P. Z. Moghadam, M. J. Lennox, F. Ragon, M. Boulhout, S. Biswas, K. G. M. Laurier, I. Beurroies, R. Denoyel, M. Roeffaers, N. Stock, T. Düren, C. Serre and D. E. De Vos, *J. Am. Chem. Soc.*, 2011, **133**, 18526–18529.
58 M. A. Moreira, J. C. Santos, A. F. P. Ferreira, J. M. Loureiro, F. Ragon, P. Horcajada, P. G. Yot, C. Serre and A. E. Rodrigues, *Microporous Mesoporous Mater.*, 2012, **158**, 229–234.
59 R. El Osta, A. Carlin-Sinclair, N. Guillou, R. I. Walton, F. Vermoortele, M. Maes, D. De Vos and F. Millange, *Chem. Mater.*, 2012, **53**, 2781–2791.
60 M. A. Moreira, J. C. Santos, A. F. P. Ferreira, J. M. Loureiro, F. Ragon, P. Horcajada, K.-E. Shim, Y.-K. Hwang, U.-H. Lee, J.-S. Chang, C. Serre and A. E. Rodrigues, *Langmuir*, 2012, **28**, 5715–5723.
61 M. A. Moreira, J. C. Santos, A. F. P. Ferreira, J. M. Loureiro and A. E. Rodrigues, *Ind. Eng. Chem. Res.*, 2011, **50**, 7688–7695.
62 M. A. Moreira, J. C. Santos, A. F. P. Ferreira, U. Müller, N. Trukhan, J. M. Loureiro and A. E. Rodrigues, *Sep. Sci. Technol.*, 2011, **46**, 1995–2003.
63 F. Millange, N. Guillou, R. I. Walton, J.-M. Grenèche, I. Margiolaki and G. Férey, *Chem. Commun.*, 2008, 4732–4734.
64 P. S. Bárcia, D. Guimarães, P. A. P. Mendes, J. A. C. Silva, V. Guillerm, H. Chevreau, C. Serre and A. E. Rodrigues, *Microporous Mesoporous Mater.*, 2011, **139**, 67–73.
65 S. Van der Perre, T. Duerinck, P. Valvekens, D. E. De Vos, G. V. Baron and J. F. M. Denayer, *Microporous Mesoporous Mater.*, 2013, **189**, 216–221.
66 T. Duerinck, R. Bueno-Perez, F. Vermoortele, D. E. De Vos, S. Calero, G. V. Baron and J. F. M. Denayer, *J. Phys. Chem. C*, 2013, **117**, 12567–12578.
67 M. Maes, F. Vermoortele, M. Boulhout, T. Boudewijns, C. Kirschhock, R. Ameloot, I. Beurroies, R. Denoyel and D. E. De Vos, *Microporous Mesoporous Mater.*, 2012, **157**, 82–88.
68 M. Maes, S. Schouteden, K. Hirai, S. Furukawa, S. Kitagawa and D. E. De Vos, *Langmuir*, 2011, **27**, 9083–9087.

69 T. Uemura, K. Kitagawa, S. Horike, T. Kawamura, S. Kitagawa, M. Mizuno and K. Endo, *Chem. Commun.*, 2005, 5968–5970.
70 T. Uemura, D. Hiramatsu, Y. Kubota, M. Takata and S. Kitagawa, *Angew. Chem., Int. Ed.*, 2007, **46**, 4987–4990.
71 Q.-K. Liu, J.-P. Ma and Y.-B. Dong, *J. Am. Chem. Soc.*, 2010, **132**, 7005–7017.
72 A. V. Morev and V. Y. Artyukhov, *Atmos. Oceanic Opt.*, 2004, **17**, 228–230.
73 Y.-Y. Fu, C.-X. Yang and X.-P. Yan, *J. Chromatogr. A*, 2013, **1274**, 137–144.
74 M. Maes, L. Alaerts, F. Vermoortele, R. Ameloot, S. Couck, V. Finsy, J. F. M. Denayer and D. E. De Vos, *J. Am. Chem. Soc.*, 2010, **132**, 2284–2292.
75 K. Hirai, S. Furukawa, M. Kondo, H. Uehara, O. Sakata and S. Kitagawa, *Angew. Chem., Int. Ed.*, 2011, **50**, 8057–8061.
76 M. E. Kosal, J.-H. Chou, S. R. Wilson and K. S. Suslick, *Nat. Mater.*, 2002, **1**, 118–121.
77 B. Kesanli and W. Lin, *Coord. Chem. Rev.*, 2003, **246**, 305–326.
78 M. Banerjee, N. R. Champness, A. I. Cooper, S. Das, R. Fischer, J.-X. Jiang, K. Kim, S. Kitagawa, W. Lin, X. Lin, L. Ma, V. Mugnaini, N. Roques, F. Schröder, T. Uemura, J. Veciana and M. Yoon, *Functional Metal-Organic Frameworks: Gas Storage, Separation and Catalysis*, 2010.
79 J. Seo, D. Whang, H. Lee, S. Jun, J. Oh, Y. Jeon and K. Kim, *Nature*, 2000, **404**, 982–986.
80 R.-G. Xiong, X.-Z. You, B. F. Abrahams, Z. Xue and C.-M. Che, *Angew. Chem.*, 2001, **113**, 4554–4557.
81 D. Bradshaw, T. J. Prior, E. J. Cussen, J. B. Claridge and M. J. Rosseinsky, *J. Am. Chem. Soc.*, 2004, **126**, 6106–6114.
82 M. Padmanaban, P. Müller, C. Lieder, K. Gedrich, R. Grünker, V. Bon, I. Senkovska, S. Baumgärtner, S. Opelt, S. Paasch, E. Brunner, F. Glorius, E. Klemm and S. Kaskel, *Chem. Commun.*, 2011, **47**, 12089–12091.
83 R. Vaidhyanathan, D. Bradshaw, J.-N. Rebilly, J. P. Barrio, J. A. Gould, N. G. Berry and M. J. Rosseinsky, *Angew. Chem., Int. Ed.*, 2006, **45**, 6495–6499.
84 D. N. Dybtsev, A. L. Nuzhdin, H. Chun, K. P. Bryliakov, E. P. Talsi, V. P. Fedin and K. Kim, *Angew. Chem., Int. Ed.*, 2006, **45**, 916–920.
85 A. L. Nuzhdin, D. N. Dybtsev, K. P. Bryliakov, E. P. Talsi and V. P. Fedin, *J. Am. Chem. Soc.*, 2007, **129**, 12958–12959.
86 Y. Song, T. Zhou, X. Wang, X. Li and R. Xiong, *Cryst. Growth Des.*, 2006, **6**, 14–17.
87 H.-X. Zhang, F. Wang, Y.-X. Tan, Y. Kang and J. Zhang, *J. Mater. Chem.*, 2012, **22**, 16288.
88 G. Xu, X. Zhang, P. Guo, C. Pan, H. Zhang and C. Wang, *J. Am. Chem. Soc.*, 2010, **132**, 3656–3657.
89 H.-Y. Kim, S.-N. Kim, J. Kim and W.-S. Ahn, *Mater. Res. Bull.*, 2013, **48**, 4499–4505.
90 O. M. Yaghi, C. E. Davis, G. Li and H. Li, *J. Am. Chem. Soc.*, 1997, **119**, 2861–2868.
91 R. Ahmad, A. G. Wong-Foy and A. J. Matzger, *Langmuir*, 2009, **25**, 11977–11979.
92 R. Ameloot, A. Liekens, L. Alaerts, M. Maes, A. Galarneau, B. Coq, G. Desmet, B. F. Sels, J. F. M. Denayer and D. E. De Vos, *Eur. J. Inorg. Chem.*, 2010, 3735–3738.
93 M. Maes, F. Vermoortele, L. Alaerts, J. F. M. Denayer and D. E. De Vos, *J. Phys. Chem. C*, 2011, **115**, 1051–1055.
94 M. Maes, F. Vermoortele, L. Alaerts, S. Couck, C. E. A. Kirschhock, J. F. M. Denayer and D. E. De Vos, *J. Am. Chem. Soc.*, 2010, **132**, 15277–15285.
95 H. Jasuja, N. C. Burtch, Y.-G. Huang, Y. Cai and K. S. Walton, *Langmuir*, 2013, **29**, 633–642.
96 P. M. Schoenecker, C. G. Carson, H. Jasuja, C. J. J. Flemming and K. S. Walton, *Ind. Eng. Chem. Res.*, 2012, **51**, 6513–6519.
97 K. A. Cychosz and A. J. Matzger, *Langmuir*, 2010, **26**, 17198–17202.
98 Y. Bai, G. He, Y. Zhao, C. Duan, D. Dang and Q. Meng, *Chem. Commun.*, 2006, 1530–1532.
99 C.-Y. Huang, M. Song, Z.-Y. Gu, H.-F. Wang and X.-P. Yan, *Environ. Sci. Technol.*, 2011, **45**, 4490–4496.
100 S. H. Jhung, J.-H. Lee, J. W. Yoon, C. Serre, G. Férey and J.-S. Chang, *Adv. Mater.*, 2007, **19**, 121–124.
101 Z. Hasan, J. Jeon and S. H. Jhung, *J. Hazard. Mater.*, 2012, **209–210**, 151–157.
102 Y. Hu, C. Song, J. Liao, Z. Huang and G. Li, *J. Chromatogr. A*, 2013, **1294**, 17–24.
103 E. Haque, J. E. Lee, I. T. Jang, Y. K. Hwang, J.-S. Chang, J. Jegal and S. H. Jhung, *J. Hazard. Mater.*, 2010, **181**, 535–542.
104 S.-H. Huo and X.-P. Yan, *J. Mater. Chem.*, 2012, **22**, 7449.
105 M. Maes, S. Schouteden, L. Alaerts, D. Depla and D. E. De Vos, *Phys. Chem. Chem. Phys.*, 2011, **13**, 5587–5589.
106 J. C. Saint Remi, T. Rémy, V. Van Hunskerken, S. van de Perre, T. Duerinck, M. Maes, D. De Vos, E. Gobechiya, C. E. a. Kirschhock, G. V. Baron and J. F. M. Denayer, *ChemSusChem*, 2011, **4**, 1074–1077.
107 X. Liu, H. Jin, Y. Li, H. Bux, Z. Hu, Y. Ban and W. Yang, *J. Membr. Sci.*, 2013, **428**, 498–506.
108 J. Cousin Saint Remi, G. Baron and J. Denayer, *Adsorption*, 2012, **18**, 367–373.

